ABSTRACT

STEBBING, RACHAEL ELIZABETH. An ITAM in a Non-enveloped Virus (Reovirus) Regulates Activation of NF-κB, Induction of Interferon-β, and Viral Spread. (Under the direction of Dr. Barbara Sherry).

Immunoreceptor tyrosine-based activation motifs (ITAMs) are signaling domains located within the cytoplasmic tails of many transmembrane receptors and within the subunits of multi-component receptor complexes. ITAMs are widely expressed throughout the immune system where they mediate activation of intracellular signaling by key immunoreceptors and have been identified in myeloid and NK cell-associated adaptor proteins DNAX-activating protein (DAP12) and Fc receptor-associated γ chain (FcRγ) in myeloid and NK cells. Furthermore, several enveloped viruses have evolved to encode ITAM-containing sequences within their genomes that participate in viral pathogenesis and oncogenesis. Here, we identified ITAM sequences in three mammalian reovirus proteins, μ2, σ2, and λ2. We demonstrate for the first time that μ2 undergoes extensive tyrosine phosphorylation, contains a functional ITAM, and activates NF-κB. Specifically, μ2 recruits the well-known ITAM-associated signaling intermediate Syk to cytoplasmic viral factories and the μ2 ITAM is required for this translocation. Moreover, both the μ2 ITAM and Syk are required for maximal μ2 activation of NF-κB. Reverse genetics was used to engineer mutant T3D reoviruses in which the two critical tyrosines in ITAMs of σ2, μ2, and λ2 were replaced with phenylalanine residues (YYFF). Tyrosine-to-phenylalanine substitutions were chosen to prevent the phosphorylation required for ITAM function and to minimally alter protein structure given the similarity of the tyrosine and phenylalanine side chains. Reovirus mutant μ2-YYFF activates less NF-κB and induces less of the downstream antiviral cytokine interferon (IFN)-β than wild type virus despite similar replication. Notably, the consequences

of these μ2 ITAM effects are cell type-specific. In non-specialized L929 cells where NF-κB is required for reovirus-induced apoptosis, the μ2 ITAM is advantageous for viral spread and enhances viral fitness. Conversely, in cardiac myocytes where the IFN response is critical for antiviral protection and NF-κB is not required for apoptosis, the μ2 ITAM stimulates cellular defense mechanisms and thereby diminishes viral fitness. These results suggest that the cell type-specific impact of the μ2 ITAM on viral spread likely reflects the cell type-specific functions of NF-κB and IFN-β. This first evidence for a functional ITAM in a non-enveloped virus presents a novel mechanism for viral ITAM-mediated signaling with likely organ-specific consequences in the host.

An ITAM in a Non-enveloped Virus (Reovirus) Regulates Activation of NF-κB, Induction of Interferon-β, and Viral Spread

by
Rachael Elizabeth Stebbing

A thesis submitted to the Graduate Faculty of
North Carolina State University
in partial fulfillment of the
requirements for the degree of
Master of Science

Comparative Biomedical Sciences

Raleigh, North Carolina

2013

APPROVED BY:

_____	_____
Dr. Barbara Sherry Committee Chair	Dr. Jeffrey A. Yoder
_____	
Dr. Fred J. Fuller	

DEDICATION

To Grandmother and Honey- my grandparents, role models, and guardian angels.

I wouldn’t be who I am today without you.

BIOGRAPHY

Rachael Elizabeth Stebbing was born and raised in Richmond, Virginia with her sister, Sarah, and brother, Todd, by their parents, Todd and Dottie Stebbing. Her grandparents, Harry and Ida Stebbing, and Barbara Waters, have also played a large role in her life. After graduating from high school in 2005, Rachael continued her education at Louisiana State University where she majored in microbiology with a minor in chemistry. Not only did she discover a passion for science, she instantly fell in love with the culture, food, and people of Louisiana, not to mention the football. A die-hard fan of both the LSU Tigers and New Orleans Saints, Rachael was lucky enough to see her teams win both a National Championship and a Superbowl during her time spent in southern Louisiana. Working in a research lab under the direction of Dr. Fred Rainey, and at the Louisiana Animal Disease Diagnostic Laboratory located at the LSU School of Veterinary Medicine, influenced Rachael to pursue a graduate degree in biomedical sciences. After graduating from LSU in 2009, she began her Master's degree at North Carolina State University under the direction of Dr. Barbara Sherry. Once in Raleigh, Rachael fell in love with another city where she spends her free time enjoying local beer and live music downtown with friends. After completing her Master's degree, Rachael plans to pursue a career in industry within the virology field.

ACKNOWLEDGMENTS

I would like to start by thanking my graduate advisor, Dr. Barbara Sherry. Her guidance and support made this work possible, and her passion and drive have been an inspiration. To all the members of the Sherry Lab, past and present, thank you for sharing late nights, invaluable discussions on our work, and for your endless encouragement. To my committee members, Dr. Jeffrey Yoder and Dr. Fred Fuller, thank you for your helpful suggestions and input on this project. I would also like to thank my undergraduate advisor, Dr. Fred Rainey, whose guidance and direction has greatly influenced the scientist I am today.

To the CVM graduate students, faculty, and staff, thank you for your constant support and for helping to make our campus feel like a home away from home. To Susan Bowman and Kelsey Poorman, thank you for not only for being there to vent to when experiments aren't working, but for reminding me that grad students can still have fun. To all my friends in Virginia, Louisiana, and North Carolina, thank you for always being just a phone call away, the memorable weekend trips and nights downtown, and for life-long friendships that can get us through anything.

I would especially like to thank my family. Their continuous love and support have helped me turn my dreams into reality. And to Carey Van, my partner in crime and the love of my life, thank you for being there with me throughout this entire process. I couldn't have done it without you.

TABLE OF CONTENTS

LIST OF FIGURES

CHAPTER 1: Literature Review

CHAPTER 2: An ITAM in a Non-enveloped Virus Regulates Activation of NF-κB Induction of Interferon-β, and Viral Spread

CHAPTER 1

Literature Review

Reovirus

Mammalian orthoreoviruses, commonly referred to as reoviruses, are nonenveloped double-stranded RNA (dsRNA) viruses belonging to the Reoviridae family. The name reovirus is derived from an acronym for **r**espiratory **e**nteric **o**rphan virus since human infections typically involve the respiratory and intestinal tracts and are not associated with severe disease (33). Three reovirus serotypes have been identified by neutralization and hemagglutination-inhibition assays. Prototypical laboratory strains of each serotype were isolated from children in the 1950s and are designated type 1 Lang (T1L), type 2 Jones (T2J), type 3 Abney (T3A), and type 3 Dearing (T3D) (1, 33, 89, 92).

Reoviruses serve as highly tractable experimental models for studies of viral replication, pathogenesis, and virus-host interactions. Following infection of neonatal mice, reoviruses disseminate systemically, inducing pathology in a variety of organs including the central nervous system, heart, and liver. Notably, tissue damage resulting from reovirus infection in this model is not attributed to immune-mediated effects, but to direct viral cytopathic effects mediated by virus-induced apoptosis and necrosis (8, 27, 33). Coinfection in mice or cultured cells allows for gene segment exchange among reovirus strains and results in a collection of reassortant viruses. Studies using reovirus reassortants have been used to correlate biological polymorphisms displayed by different reovirus strains with specific virus gene segments, and to identify viral determinants of tropism and disease in the central nervous system and heart (33, 98). More recently, a plasmid-based reverse genetics system for mammalian reoviruses was developed. Using this system, specific mutations can

be engineered into virion capsid and nonstructural proteins to create viruses containing specific sequence modifications. Reverse genetics has provided the necessary tool to enhance studies of viral replication and pathogenesis, and can be exploited to engineer recombinant viruses for vaccine and oncolytic applications (10, 33, 59).

Reoviruses form icosahedral virions consisting of two concentric protein shells, the inner core and outer capsid, surrounding a 23.5kb genome encoded by 10 discontiguous segments of dsRNA (28, 33). The genome segments are named by size according to their migration on polyacrylamide gels. There are three large segments (L1, L2, and L3), three medium segments (M1, M2, and M3), and four small segments (S1, S2, S3, and S4) (28, 33, 97). The 10 segments of the Reovirus genome encode 12 proteins which are denoted by a Greek symbol corresponding to the large (λ), medium (μ), and small (σ) genome segments; however, the numbering of the gene segments does not always correspond to the numbering of the proteins. Each dsRNA segment encodes a single protein, except for the S1 and M3 gene segments which encode a second protein as a product of alternative translation. Of the 12 reovirus proteins, eight are structural (λ1, λ2, λ3, μ1, μ2, σ1, σ2, and σ3) and four are nonstructural (μNS, μNSC, σ1s, and σNS) (33). In addition to genomic dsRNA segments, reovirus virions contain short, single-stranded RNA oligonucleotides. These RNA oligos are a result of aborted transcription and while there is evidence they are dispensable for infectivity, their significance is still not entirely understood (7, 36, 96).

Viral Entry

Viral attachment protein σ1, encoded by the S1 gene segment, mediates binding to cell-surface receptors and influences distinct disease patterns of reovirus serotypes (33, 91).

Additionally, σ1 has been identified as the viral protein responsible for hemagglutination (15). The trimeric protein complex is composed of a globular carboxy-terminal tail, a central body, and a filamentous amino-terminal tail. σ1 is anchored at each of the icosahedral vertices and extends from pentameric turrets formed by the L2-encoded λ2 protein. Reovirus attachment proceeds via a two-step adhesion-strengthening mechanism. The σ1 body engages widely distributed cell-surface glycans with low affinity, and is followed by high affinity binding of the σ1 head to immunoglobulin superfamily member, junctional adhesion molecule-A (JAM-A) (4, 5, 55, 91). Following receptor binding, reovirus utilizes β1 integrins to mediate internalization of the particle, most likely through clathrin-dependent endocytosis (69, 71). During the entry process, reovirus particles are sorted into vacuoles resembling endosomes and lysosomes where they undergo proteolytic disassembly. Studies have found that both NPXY motifs in the β1 integrin cytoplasmic tail and Src kinase play a role in targeting reovirus particles to endocytic organelles containing GTPases Rab7 and Rab9 (70-72) . It was also recently reported that reovirus virions colocalize with microtubules and microtubule motor dynein 1 following internalization, and that functional microtubules are required for proper sorting of reovirus virions (73). Within minutes of internalization, reovirus virions undergo stepwise disassembly to form well defined intermediates, the first being the infectious subvirion particle (ISVP). ISVPs are characterized by the loss of S4-encoded, outer capsid protein σ3 and cleavage of M2-encoded, outer capsid protein μ1 to form μ1δ and φ (28, 70). The rate-limiting step in reovirus disassembly is the proteolytic removal of σ3, which in fibroblasts is dependent on acidic pH and the endosomal cysteine-containing proteases, cathepsins B and L (35, 70, 100). A recent study has implicated

interferon-inducible transmembrane protein IFITM3 in restriction of reovirus entry through alteration of endosomal function either by delaying acidification or modulating proteolytic processing of virions (3). Following ISVP formation, σ1 is shed and the μ1δ fragment undergoes conformational rearrangement to yield ISVP*. During ISVP* formation, the autocatalytic cleavage of μ1δ also occurs, generating the N-terminal myristoylated peptide μ1N (2, 27). Both μ1N and φ are released from the ISVP*s and play a role in pore formation (49). While transition to ISVP* is associated with membrane penetration, the mechanism for the release of viral cores into the cytoplasm is not fully understood. The timing remains unclear, however, molecular chaperone Hcs70 has been found to play a role in the release of the δ fragment from ISVP* to complete outer capsid disassembly and generate a transcriptionally active reovirus core (48).

Viral Replication

Reovirus core particles contain the genome and enzymatic machinery required for synthesizing and exporting viral mRNA into the cytoplasm of infected cells. Core protein λ1, encoded by the L3 gene, is a major component of the shell surrounding the viral genome, and defines the symmetry and size of the reovirus core particle (90). Evidence that λ1 contains a putative nucleotide-binding motif, exhibits an affinity for nucleic acids, and mediates helicase activity, support the idea that it plays a role in transcription of the viral genome (9). The second major core protein σ2, encoded by the S2 gene, binds at three locations within each icosahedral asymmetric unit, serving as a stabilizing clamp (90). L1-encoded, minor core protein λ3 is the RNA-dependent RNA polymerase (RdRp) and has been localized beneath the λ1 shell at each of the five-fold axes (99, 110). The specific role and location of

M1-encoded, minor core protein μ2 within viral cores remain unclear. Evidence for μ2 binding RNA, exhibiting NTPase and RTPase activities, and interacting with the λ3 polymerase suggests μ2 plays a role in viral mRNA synthesis (12, 54, 81). The role of μ2 in reovirus infection will be discussed in greater detail in a subsequent section of this literature review. Projecting from the λ1 shell, core spike protein λ2 forms turrets around each of the icosahedral five-fold axes (90). During primary transcription within the core, positive-sense ssRNA is synthesized from negative-strand templates of the genomic dsRNA. Nascent ssRNA is extruded through the λ2 turrets, where guanylyltransferase and methyltransferase activity mediate the addition of a 5' cap before release of the transcript into the cytosol (21, 33). Following extrusion into the cytoplasm, the primary transcripts serve as both mRNA for translation of viral proteins, and as templates for negative-strand synthesis (78). The replication and assembly of reovirus progeny occurs within cytoplasmic structures termed viral factories (VFs), also known as viral inclusion bodies. The inclusions lack a delimiting membrane and contain viral proteins, dsRNAs, and particles at various stages of morphogenesis (77, 83). VFs are hypothesized to mediate progeny virus replication and assembly by sequestering and concentrating viral RNA and proteins. It is also possible that VFs function to mask viral RNA from recognition by intracellular pattern-recognition receptors (33). Studies of both VFs in infected cells and viral factory-like structures formed by ectopically expressed protein have implicated the M3-encoded, nonstructural protein μNS in viral factory formation. μNS initiates VF formation by establishing a structural matrix and acting as a scaffolding protein for recruitment of μ2, S3-encoded nonstructural protein σNS, and core structural proteins λ1, λ2, and λ3 (13, 77, 78). Studies using siRNA found that viral

proteins μ2, μNS, and σNS are each involved in VF formation and maturation and are indispensable components of reovirus replication (16, 57). VFs become tethered to the cellular cytoskeleton via μNS associations with the microtubule-associated viral protein μ2. This association allows VFs to travel toward the nucleus and merge with other VFs, ultimately forming the large perinuclear inclusions characteristic of reovirus infected cells (77, 86). The final step in virion assembly is completed by the addition of outer capsid proteins to core particles. While the specific mechanism is unclear, the release of newly synthesized reovirus particles from infected cells is likely facilitated by cellular lysis and reovirus-induced apoptosis (33).

Apoptosis

Programmed cell death, or apoptosis, is induced by the activation of caspases through either the intrinsic or extrinsic pathway. The intrinsic pathway is initiated when Bcl-2 family members sense cellular stress and insert into the mitochondrial membrane (26). Following insertion, cytochrome c and Smac/DIABLO are released from the mitochondria into the cytosol, and caspase-9 is activated. Cytochrome c, caspase-9, and Apaf-1 form a large protein complex termed the apoptosome. Finally, the apoptosome activates caspase-3 and caspase-7 to execute the final stages of the apoptotic response (26). In contrast, the extrinsic pathway is activated by ligation of extracellular ligands to transmembrane receptors containing death domains (26). Receptor activation results in the formation of a death inducing signaling complex (DISC) and subsequent activation of caspase-8. Depending on cell type, caspase-8 either directly activates caspase-7 and caspase-9, or requires further amplification of death signals through Bid stimulation of the mitochondrial pathway (26).

Reovirus infection leads to the induction of apoptosis in a variety of cell types, and correlates with pathology in vivo as the mechanism of virus-induced tissue injury. Studies suggest that both death receptor and mitochondrial pathways play an essential role in mediating reovirus-induced apoptosis (Fig. 1.1) (60). Additionally, reovirus-induced apoptosis is regulated by the activation of transcription factor NF-κB, and requires both IRF-3 and IPS-1 for efficient induction of apoptosis following infection (24, 44). The role of NF-κB in reovirus infection will be discussed in greater detail in a subsequent section of this literature review.

Defined mechanisms by which reovirus infection triggers apoptosis are unknown; however, genetic studies have identified the μ1-encoding M2 gene as a viral determinant of apoptosis (27, 30). Reovirus strains differ in their ability to induce apoptosis, with T3D inducing significantly higher levels of apoptosis than TIL. When originally investigating strain-specific differences in induction of apoptosis, the σ1-encoding S1 gene was hypothesized to be the primary determinant of apoptotic (23, 24, 103). It was later found that signaling pathways activated by binding of σ1 to JAM-A and sialic acid are dispensable for reovirus-mediated apoptosis, and that μ1 is the principal viral factor for stimulation of cellular apoptotic machinery (29). The importance of μ1 in reovirus-induced apoptosis has been demonstrated in both genetic and in vivo studies. Small, defined regions within the C-terminal portion of μ1 were identified as key determinants for induction of apoptosis, and in both reovirus infected and transfected cells, μ1 was found to localize to lipid droplets, ER, and mitochondria (22). In another study, the μ1 φ domain was identified as a key regulator in membrane penetration and subsequent stimulation of apoptosis (27). Furthermore, mutant

viruses harboring a membrane-penetrative defective μ1 protein were found to have an attenuated capacity to produce encephalitis and resulted in decreased activation of NF-κB and IRF-3 (30).

As part of the extrinsic pathway, reovirus induces the release of tumor necrosis factor (TNF)-related apoptosis-inducing ligand (TRAIL) and upregulation of TRAIL-associated death receptors (DRs) DR4 and DR5 in infected cells. Reovirus-induced apoptosis can be blocked with anti-TRAIL antibody or with soluble forms of DR4 and DR5, demonstrating that signaling via death receptors is required for execution of apoptosis (19). DR activation is followed by activation of caspase-8 and subsequent cleavage of the pro-apoptotic Bcl-2 family member, Bid, into its truncated form, tBid (60). tBid translocates to the mitochondria and triggers the release of cytochrome c, effectively linking the extrinsic apoptotic pathway and the mitochondrial amplification loop of the intrinsic pathway. Studies have found that while Bid is dispensable for reovirus replication, NF-κB-dependent cleavage of Bid is required for reovirus-induced apoptosis (31).

Demonstrating the use of the intrinsic pathway, reovirus infection induces the release of cytochrome c and Smac/DIABLO from the intermitochondrial space, and the activation of caspase-9 (60). Mirroring reovirus-induced apoptosis, ectopic expression of μ1 stimulates the release of cytochrome c and Smac/DIABLO into the cytosol, and the activation of both caspases 8 and 9 (Fig. 1.1) (106). Furthermore, reovirus-induced apoptosis was found to occur independently of the proapoptotic Bcl-2 family members Bax and Bak, suggesting additional BH3-only proapoptotic proteins may be involved in reovirus-induced cytochrome c release. Insertion of tBid into the mitochondrial membrane is mechanistically similar to that

of Bax and Bak, supporting the hypothesis that tBid can substitute for Bax and Bak to permeabilize mitochondrial membranes for the subsequent release of cytochrome c and Smac/DIABLO. It is also possible that μ1 itself can directly permeabilize mitochondrial membranes (106). Additionally, the proapoptotic BH3-only protein NOXA was found to be upregulated following reovirus infection in an IRF-3 and NF-κB dependent manner. In cells lacking NOXA, the level of reovirus-induced apoptosis was significantly diminished, indicating a critical function for NOXA in efficient induction of apoptosis by reovirus (56).

Reovirus Protein μ2

The reovirus M1 genome segment is 2,304 base pairs in length and contains a single long open reading frame encoding the 736 amino acid protein μ2 (Fig. 1.2) (111). The 83-kDa μ2 protein is a structurally minor component of the reovirus core, found in low copy numbers (~20 copies per viral particle) near the icosahedral fivefold vertices. Being the only structural protein for which no crystal structure is available, μ2 is the most functionally and structurally enigmatic of the reovirus proteins (54, 108). M1 genome segment sequences have been determined for the three prototypic reoviruses T1L, T3D, and T2J. The M1 gene of strains T1L and T3D demonstrate a high degree of conservation, sharing ~98% nucleotide sequence homology and ~99% amino acid sequence homology, one of the highest values seen between reovirus genome segments from distinct isolates (108, 111). In contrast, the T2J strain shares only ~71% nucleotide sequence homology and ~80% amino acid sequence

homology with T1L and T3D (108). Sequence comparisons of 12 reovirus isolates identified eight highly conserved regions within μ2, each containing at least 15 consecutive amino acids identical in all isolates. The regions are further clustered in two larger areas spanning amino acids 1-250 and 400-610 (108). The same study also suggests that the μ2 protein can be divided into four regions distinguished by varying patterns of predicted secondary structure. A highly conserved amino-terminal region spans amino acids 1 through 157 and is predicted to contain six α-helices and three β-sheets (108). A variable region, spanning amino acids 157 through 450, is predicted to be the most structurally complex region, consisting of multiple interspersed α-helices and β-sheets (108). A second highly conserved region referred to as a helix rich region spans amino acids 450 through 606 and contains seven α-helices (108). The carboxyl-terminal region spans remaining amino acids 606 through 736 and is the least conserved region as it varies across all three reovirus serotypes (108). The overall predicted composition of μ2 is 48% α-helix and 14% β-sheet, classifying it as an α-β protein (108). Computer-based comparisons of the highly conserved regions of μ2 with sequences in protein data banks fail to show significant homology to other proteins, substantiating the uniqueness of this viral protein. Matching with less than 90% certainty, the SH2 domain of tyrosine kinases received the highest score, with four of five motifs in the SH2 domain matching the μ2 sequence (108). Interestingly, most tyrosine kinases with SH2 domains are also classified as α-β proteins. Given that SH2 domains mediate protein-protein interactions, these results suggest that μ2 may function similarly (108). It is important to note that Src family kinases and Syk family kinases also contain SH2 domains, as they will be discussed further in a subsequent section of this literature review.

The specific role of minor core protein μ2 in reovirus replication remains poorly defined; however, siRNA studies have found that inhibition of μ2 substantially diminishes viral dsRNA synthesis, protein production, and VF formation, indicating μ2 functions as a critical component of the viral replication machinery (16, 57). As previously mentioned, μ2 is able to bind ssRNA and dsRNA and exhibits both nucleoside and RNA triphosphatase activities that are enhanced by the presence of RdRp λ3 (12, 54, 81). Investigation of μ2 functional domains revealed a dependence of viral replication on μ2 NTPase/RTPase functionality as a result of intact Walker A- and B-like motifs (58). The same study also identified a functional nuclear localization motif within a cluster of N-terminal basic residues as critical for viral replication and suggest that nuclear targeting of μ2 is required for completion of the infectious cycle (58).

Providing additional evidence for a role of μ2 in transcription, studies using reassortant viruses have demonstrated that the M1 gene segment segregates with strain-specific differences in the temperature optimum of transcription in vitro as well as the total number of transcripts produced (107). A cell type-specific role for the M1 gene in reovirus replication efficiency has been demonstrated in cardiac myocytes and L929 cells. In cardiac myocytes, the difference in the capacity for different viral strains to grow was mapped to the M1, L1, and L3 genes, while in L929 cells only the L1 and L3 genes were implicated (75). Furthermore, μ2 has been identified as the primary determinant for strain-dependent replication efficiency in bovine aortic endothelial cells and in Madin-Darby canine kidney (MDCK) cells (74, 84). Upon further investigation it was determined that a sequence polymorphism at amino acid position 347 was found to regulate μ2-mediated reovirus

growth in MDCK cells in a temperature-dependent manner, and that regulation occurs subsequent to inclusion development and prior to formation of genomic dsRNA . These observations suggest that virion particle assembly is a µ2-regulated step and may represent an unidentified role for µ2 in virion morphogenesis (83, 84).

Following primary transcription and translation, µ2 is recruited in high concentrations to viral factories. VF morphology is reovirus strain-dependent with T1L forming filamentous inclusions and T3D forming globular inclusions (86). Strain-dependent differences in the kinetics of inclusion formation and inclusion morphology are determined by the M1 gene, specifically amino acid 208 (76, 86). Recent studies have also implicated amino acid 383 in modulation of VF morphology (58). As previously described, nonstructural protein µNS initiates VF formation and recruitment of viral proteins, including µ2. Neither µ2 nor µNS can form mature filamentous inclusions in the absence of the other, indicating a requirement for additional protein(s) to form mature inclusions (13). Studies found that µ2 proteins from reoviruses that induce filamentous inclusions bind to and stabilize microtubules (MTs) as indicated by hyperacetylation of α-tubulin, implicating µ2 as a viral MT-associated protein (MAP) (13). Colocalization of µNS and µ2 is independent of reovirus strain-specific differences; however, µNS-µ2 association with MTs, and ultimately VIB morphology, is dependent on strain-specific differences in reovirus protein µ2 (13). In T3D infected cells, µNS binds to viral cores and incorporates them into inclusions to form globular VFs. In T1L infected cells, cores bound by µNS are recruited to MTs through the µNS-µ2 association to form filamentous VIBs (13). Evidence that µ2 from reovirus strains that generate globular VFs form aggregates with little association with MTs in the absence of other viral proteins

suggest it may misfold (86). Upon investigation, it was found that μ2 proteins from strains generating globular VFs display higher levels of ubiquinated μ2 than those from strains generating filamentous VFs, and that strains that form globular VFs at 37°C shows increased formation of filamentous VFs and decreased colocalization with ubiquitin at 31°C (79). These results suggest that μ2 from globular reovirus strains is prone to temperature-dependent misfolding which leads to increased aggregation, increased ubiquitination, and decreased association with MTs. Strain-specific differences in ubiquitination were mapped to amino acid 208, providing further evidence for a key role of residue 208 in influencing reovirus protein μ2 (79).

The M1 gene has also been implicated in viral subversion of the interferon response (47, 112). Reovirus represses the interferon (IFN)-α/β signaling pathway in a strain specific manner that correlates with induction of myocarditis through a novel mechanism involving TIL μ2-induced accumulation of interferon regulatory factor 9 (IRF9) in the nuclear fraction (112). It was recently reported that μ2 amino acid 208 is the primary determinant for strain-specific repression of IFN-β signaling (47). Additionally, μ2 amino acid 208 was identified as a determinant of viral spread and tissue damage in cardiac myocytes and reovirus-induced myocarditis (47). Chapter 2 of this thesis will address a novel role of reovirus protein μ2 as an ITAM containing protein.

Nuclear Factor-Kappa B (NF-κB)

The nuclear factor-kappa B (NF-κB) family of transcription factors play an evolutionarily conserved role in the immune system and broadly influence genes involved in cell differentiation, proliferation, and death. Belonging to the Rel domain-containing protein family, there are five mammalian NF-κB subunits: RelA/p65, RelB, c-Rel, p105/NF-κB1 which is cleaved into p50, and p100/NF-κB2 which is cleaved into p52 (43, 88). NF-κB proteins exist as homodimers or heterodimers, with subunit dimerization supported by the binding of conserved N-terminal Rel homology domains (RHDs). RHDs are also responsible for DNA binding and possess a nuclear localization signal (NLS). Additionally, NF-κB proteins RelA/p65, c-Rel, and RelB contain a C-terminal transactivation domain (TAD) that mediates transcription initiation (17, 43). NF-κB dimers are held in an inactive state within the cytoplasm through association with members of the inhibitory IκB protein family. The IκB family consists of eight proteins with IκBα being the prototypical and most well studied member of the family (34, 43). Phosphorylation of IκBα on conserved destruction box serine residues S32 and S36 by IκB kinases (IKKs) leads to IκBα polyubiquitination, degradation, and subsequent release of NF-κB. Release from IκB reveals the NF-κB NLS, allowing NF-κB to accumulate in the nucleus and bind to DNA κB sites in promoters and enhancers of target genes (34, 43, 109).

NF-κB signaling occurs through two pathways depending on the activation of IKK subunits (Fig. 1.3). In the classical or canonical pathway, cell stimulation through ligand recognition by cytokine receptors (ie. TNF receptor), pattern recognition receptors (ie. Toll-

like receptors), and antigen receptors (ie. T cell receptor), among other stimuli, trigger activation of IKKβ. IKKβ associates with IKKα and the IKKβ regulatory protein NEMO/IKKγ to form a functional cytokine-responsive IKK complex. Subsequent phosphorylation of IκBα and p105/NF-κB1 results in IκBα degradation and cleavage of p105/NF-κB1 to form the NF-κB subunit p50 (43, 88, 109). In the alternative or noncanonical pathway, stimulation of specific immune cytokine receptors (ie. CD40) activate IKKα and signaling is independent of NEMO/IKKγ. Instead, NF-κB inducing kinase (NIK) activates IKKα, resulting in phosphorylation and cleavage of p100/NF-κB2 to form the NF-κB subunit p52. NF-κB subunits p50 and p52 associate with NF-κB subunits RelA/p65 and RelB, respectively, and translocate to the nucleus where NF-κB can both positively and negatively regulate gene transcription (43, 88, 109). Microbial pathogens stimulate NF-κB activation and subsequent induction of antimicrobial pro-inflammatory cellular response genes; however, the NF-κB signaling cascade is frequently targeted by pathogens for subversion of immune mediators and continued survival (88). The remainder of this section will address the activation and outcome of NF-κB signaling and mediation during reovirus infection.

Reoviruses stimulate cellular responses leading to the activation of NF-κB via recognition by RIG-I-like receptors. Following receptor engagement, signaling through the adaptor protein MAVS (also known as IPS-1, VISA, and Cardif) leads to activation of IKKs (44). Additionally, it has been demonstrated that reovirus activation of NF-κB can occur independent of RIG-I and MAVS. In the same study, reovirus protein μ1 was found sufficient to induce apoptosis when ectopically expressed, suggesting μ1 plays a role in

reovirus-induced NF-κB activation (22). It has been hypothesized that reovirus μ1 φ domain may contribute to NF-κB activation through direct or indirect stimulation of IKKs in a fashion similar to that seen during human T-lymphotropic virus (HTLV) infection, where the HTLV Tax protein stimulates IKK activity though direct interaction with NEMO/IKKγ (27). An additional mechanism of reovirus-induced NF-κB activation will be discussed in Chapter 2.

During reovirus infection, select components of both the classical and alternative NF-κB signaling pathways are required for NF-κB activation, which occurs in a biphasic pattern. Implicating use of the classical pathway, nuclear translocation of NF-κB complexes containing p50 and RelA/p65 subunits are detectable 2-8 hours post infection, followed by complexes containing p50 and c-Rel subunits detectable 8 hours post infection (24, 41). The alternative pathway of NF-κB signaling is engaged 16-24 hour post infection as detected by nuclear localization of NF-κB complexes containing p52 and RelB subunits, though it is unlikely this delayed response contributes to primary apoptotic signaling (41). Consistent with findings of nuclear translocation of NF-κB subunits p50 and RelA/p65, IκBα levels are significantly reduced by 4 hours post infection, indicating IκBα as a primary cellular target of reovirus (41). Furthermore, studies using siRNA and cells deficient in specific IKK subunits found that IKKα but not IKKβ is required for reovirus-induced NF-κB activation. Surprisingly, NF-κB activation and subsequent apoptosis was attenuated in cells lacking IKKβ regulatory subunit NEMO/IKKγ, while NIK, the protein typically responsible for IKKα activation, was found to be dispensable (41). These data support the idea that reovirus infection triggers NF-κB activation through a novel mechanism involving IKKα and

NEMO/IKKγ, IκBα proteolytic degradation, and nuclear translocation of NF-κB complexes containing p50 and RelA/p65 subunits (Fig. 1.3) (41).

The requirement for NF-κB activation in reovirus-induced apoptosis has been demonstrated by evidence that reovirus-induced apoptosis is significantly diminished in the presence of a proteosome inhibitor, in cells expressing a form of IκB that constitutively represses NF-κB, and in cells deficient for either p50 or RelA/p65 subunits (24). Additionally, a second phase of NF-κB regulation, in which NF-κB activity is inhibited, was found to be essential for efficient induction of apoptosis during reovirus infection (20). This inhibition phase occurs at late times post-infection and is characterized by a block in NF-κB activation as a result of decreased IκBα degradation. NF-κB inhibition sensitizes cells to TRAIL-mediated apoptosis, allowing both TRAIL and reovirus-induced apoptosis to occur in TRAIL-resistant cells, and links NF-κB activation to the extrinsic pathway of apoptosis (20). The reovirus S1 gene segment determines the ability of reovirus strains to initiate the NF-κB inhibition phase. This phase is also associated with apoptosis following reovirus infection of HEK293 cells and primary cardiac myocytes, and therefore contributes to viral pathogenesis (18). Additional studies implicate NF-κB as an essential mediator of the intrinsic pathway of apoptosis during reovirus infection. NF-κB activation is required for cleavage of Bcl-2 family member Bid to generate tBid. tBid translocates to the mitochondria where it amplifies the mitochondrial loop of the intrinsic pathway (31). Furthermore, proapoptotic BH3-domain only protein NOXA is strongly induced 36-48 hours post infection in a manner dependent on IRF-3 and NF-κB. Apoptosis is significantly diminished in cells lacking NOXA, indicating it as a key molecule in reovirus-induced apoptosis (56).

NF-κB mediates reovirus-induced apoptosis and subsequent pathogenesis in an organ/cell type-specific manner by either enhancing or preventing cell death signaling. Specifically, NF-κB subunit p50 was identified to play an essential role in the development of encephalitis and myocarditis in reovirus-infected mice (82). NF-κB plays a proapoptotic role in the brain. Wild-type mice exhibit significant neuronal apoptosis following reovirus infection, while despite replicating to equivalent titers, mice lacking NF-κB subunit p50 display a minimal apoptotic response (82). Following reovirus infection of the heart, NF-κB activation leads to induction of innate immune mediators, importantly IFN-β, and attenuation of viral replication. Apoptosis and disease are subsequently diminished, suggesting NF-κB mediates a protective response again reovirus infection in the heart (82). The cell type-specific roles of NF-κB during reovirus infection will be examined further in Chapter 2.

Immunoreceptor Tyrosine-Based Activation Motifs (ITAMs)

The primary focus of my contribution to the work presented in Chapter 2 pertains to a newly identified immunoreceptor tyrosine-based activation motif (ITAM) within reovirus protein μ2 (Fig. 1.2). In this section I will discuss ITAM-mediated cellular signaling and the functions of previously described viral ITAMs.

ITAMs are characterized by two critical tyrosine (Y) residues within the canonical motif YxxI/Lx_{6-12}YxxI/L, where two repeats of tyrosine-containing sequences are separated by a span of any six to twelve amino acids (x), and each tyrosine is separated by any two

amino acids from a conserved isoleucine (I) or leucine (L). Often found in multiples, ITAMs are characteristically located within the cytoplasmic tail of transmembrane receptors and within the subunits of multi-component receptor complexes (63, 104). ITAMs are widely expressed throughout the immune system where they mediate activation of intracellular signaling by key immunoreceptors including T cell receptors (TCRs), B cell receptors (BCRs), and Fc receptors (FcRs) (45, 104). In myeloid and natural killer (NK) cells, this highly conserved motif has been identified in adaptor proteins DNAX-activating protein (DAP12) and Fc receptor-associated γ chain (FcRγ). These ITAM-containing signaling chains associate through charged amino acid residues with various myeloid and NK-specific receptors to form multi-subunit complexes and initiate signaling cascades involved in cell differentiation, maturation, activation, and survival (45, 64, 101).

Engagement of ITAM-associated receptors leads to phosphorylation of ITAM tyrosine residues by Src family kinases (Fig. 1.4). Src family kinases include Src, Lck, Lyn, Fgr, Hck, Fyn, and Yes (104). Src kinases are localized to the plasma membrane through a motif within an acetylated N-terminal domain, and also contain an SH3 domain, an SH2 domain, a kinase domain, and a regulatory C-terminal tail domain. Src is held in an inactive state through phosphorylation of a C-terminal tyrosine by C-terminal kinase (Csk), which stimulates an intramolecular interaction between the tail domain and the SH2 domain of Src. The mechanism of Src activation remains poorly understood; however, removal of the phosphate by cellular phosphatases and autophosphorylation of the kinase domain prepare Src for association with stimulated receptors (11, 104). Phosphorylation of ITAM tyrosine residues leads to recruitment of spleen tyrosine kinase (Syk) (Fig. 1.4). The 72 kDa tyrosine

kinase is highly expressed in hematopoietic cells and has also been shown to be expressed in nonhematopoietic cells including fibroblast, epithelial cells, hepatocytes, neuronal cells, and vascular endothelial cells. Mammals also express the Syk homologue ZAP-70; however, expression is confined to T cells and NK cells (11, 80). Syk contains two tandem SH2 domains separated by an inter-SH2 domain linker, a kinase-SH2 domain linker, and a C-terminal kinase domain. Phosphorylation of Syk tyrosine residues 348/352 within the SH2 domain and 525/526 within the activation loop of the kinase domain have been identified to regulate Syk activity and serve as docking sites for other proteins. Interaction of Syk SH2 domains with ITAM phosphotyrosines stimulates Syk autophosphorylation and initiates downstream signaling cascades that result in a variety of cellular responses (Fig. 1.4) (80, 94, 102). Effector molecules and transcription factors of importance activated during or in response to ITAM-mediated signaling include phospholipase-Cγ (PLCγ), protein kinase C (PKC), phosphatidylinositide 3-kinase (PI3K), mitogen-activated protein kinases (MAPKs), activator protein 1 (AP-1), nuclear factor of activated T cells (NFAT), and NF-κB (Fig. 1.4) (42, 50).

Integrated crosstalk between ITAM signaling networks and other signal transduction pathways provide regulation and fine tune activation of specific cellular responses. Studies found that maximal activation of macrophages requires synergy between ITAM signaling intermediates and the IFN-α cytokine pathway. In IFN-γ primed macrophages, enhanced IFN-α-induced STAT-1 activation was found to be dependent on Syk (101). It is hypothesized that IFN-γ upregulates expression of STAT1 and induces expression of FcRγ/DAP12-coupled receptors that interact with the interferon-α/β receptor (IFNAR) to

mediate coupling of Syk to IFNAR. In the proposed model, IFNAR-associated Syk may maximize IFN-α-induced STAT-1 activation through direct phosphorylation of STAT1 or through phosphorylation of new STAT1 docking sites, subsequently increasing recruitment of STAT1 to the receptor (101). Activation of cellular networks through ITAM-mediated signaling cascades has been well documented; however, ITAMs can also mediate inhibitory signals and attenuate signaling of other receptors (40, 50). FcRγ has been shown to cross-inhibit signaling from several other receptors including Fc receptors, tumor necrosis factor receptors (TNFRs), and toll-like receptors (TLRs). One study found FcRγ in association with IgA-specific Fc receptor (FcαRI) inhibits IgG-mediated phagocytosis in monocytes and IgE-mediated degranulation in mast cells (40, 50). Additionally, preligation of ITAM-coupled β2 integrins was found to inhibit TLR induction of the IFN-β-mediated autocrine loop as well as exogenous IFN-α signaling. Studies investigating the mechanisms involved in this inhibition found that IFN-induced janus kinase 1 (Jak1) tyrosine phosphorylation is suppressed through MAPK-dependent induction of IFNAR signaling inhibitors (46). Integrated signaling between ITAM-associated receptors and TLRs has also been found to activate downstream signaling intermediates in an additive fashion, resulting in enhanced cellular responses (50). In several experimental systems, ITAM-coupled receptors have been shown to generate both positive and negative signals, though the molecular basis for this switch is not well understood. Depending on the microenvironment, DAP12 association with triggering receptor expressed on myeloid cells (TREM) can either augment or inhibit TLR-mediated cytokine production (50). Furthermore, there is a growing body of evidence supporting the idea that ITAM-mediated signaling is self-regulated through association of phosphorylated

ITAMs with inhibitory proteins. FcRγ has been found in association with Src homology region 2 domain-containing phosphatase-1 (SHP-1) following FcαRI ligation, SHP-2 has been found in associate with the FcεRI β-chain following receptor clustering, and phosphopeptides based on known cellular ITAMs have been shown to immunoprecipitate SH2 domain-containing inositol 5'-phosphatase (SHIP) (104).

Viral ITAMs

Interestingly, viruses have evolved to encode ITAM-containing sequences within their genomes that participate in viral pathogenesis and oncogenesis through mediation of traditional cellular ITAM signaling intermediates (63).

Epstein-Barr virus (EBV) is a widespread γ-herpesvirus capable of infecting both lymphoid and epithelial cells and is associated with the development of several human cancers including Burkitt's lymphoma, Hodgkin's lymphoma, gastric carcinoma (GC), and nasopharyngeal carcinoma (NCP) (37, 51, 95). EBV establishes latency in B cells, during which time latent membrane protein (LMP2) is expressed. LMP2 exists in two promoter-dependent forms, LMP2A and LMP2B, that differ in only one exon comprising a noncoding region in LMP2B and an N-terminal region in LMP2A (95). LMP2A is a highly hydrophobic protein containing twelve transmembrane domains and is localized within aggregates to the plasma membrane of latently infected B cells. Extending into the cytoplasm, the LMP2A N-terminal tail contains several signaling motifs including an ITAM surrounding tyrosine residues 74 and 85 (95). LMP2A has been implicated in maintenance of viral latency through interference of BCR signaling, which in turn blocks viral reactivation. LMP2A also contributes to the malignant phenotypes seen in both B cells and epithelial cells through

manipulation of cellular networks involved in transformation, migration, and differentiation (37). The recruitment of kinases to LMP2A ITAM residues for tyrosine phosphorylation is stimulated through cellular adhesion rather than ligand binding, and is cell type-specific. In B cells, LMP2A preferentially associates with Src family kinases Lyn and Fyn, while in epithelial cells tyrosine phosphorylation is mediated independently of Src by Csk (14, 95). Following ITAM phosphorylation, Syk is recruited and activated in a manner dependent on LMP2A tyrosine residues 74 and 85 (67). While investigating the role of LMP2A during EBV infection, Syk was found to promote LMP2A-induced epithelial cell migration through MAPK extracellular signal-regulated kinase (ERK) activation (67). Recent studies also identified the ITAM-bearing protein as essential for ERK-mediated reduction of anoikis, a type of apoptosis associated with cell detachment (51). Finally, LMP2A ITAM-mediated Syk autophosphorylation initiates Akt activation, a serine/threonine protein kinase involved in cellular survival and proliferation signaling cascades. Akt signaling contributes to B cell survival and is required for LMP2A-induced transformation of epithelial cells, further highlighting the importance of ITAM-mediated signaling in the development of EBV-induced diseases (37).

Two additional human herpesviruses that encode ITAM-containing proteins are Kaposi's sarcoma-associated herpesvirus (KSHV) and closely related rhesus monkey rhadinovirus (RRV) (25, 66). Based on epidemiological and histopathological evidence, KSHV is strongly suggested to be an etiological agent of Kaposi's sarcoma (KS), a multifocal angiogenic neoplasm. Seroprevalence of the virus varies worldwide with the highest rates of infection found in the Mediterranean basin and Africa where up to half of the

population is infected and KS is often the most common form of cancer, especially in immunecompromised individuals (65, 87). KSHV is also implicated in primary effusion lymphoma (PEL) and multicentric Castleman's disease, both rare B cell lymphoproliferative disorders. Unlike most cancers which are caused by clonal expansion of transformed cells, KS is a result of hyperplastic growth associated with local production of inflammatory cytokines. Over the course of infection, KSHV predominantly exists in a latent state, with lytic replication occurring in only a small subset of cells. Viral DNA and transcripts are present in KS spindle cells, endothelial cells identified as primary tumor cells, as well as in peripheral blood mononuclear cells (PBMCs) of infected individuals (61, 65). ITAMs have been identified within the cytoplasmic tails of KSHV transmembrane protein K1 and distantly related RRV transmembrane protein R1. Further investigation found that the K1 ITAM is able to constitutively induce signal transduction through ligand-independent activation attributed to the K1 cysteine-rich extracellular domain (25, 62, 66). The Src family kinase Lyn is recruited to the K1 ITAM, resulting in subsequent ITAM tyrosine phosphorylation and recruitment of Syk. K1 ITAM-dependent signaling was found to be dispensable for viral reactivation in KS spindle cells which lack Syk, but can augment replication and signaling in cells competent for ITAM signaling such as B cells (61). Furthermore, the K1 ITAM interacts with additional cellular SH2-containing proteins including the p85α regulatory subunit of PI3K, PLCγ2, and Vav. Mutational analysis demonstrated that each K1 ITAM tyrosine residue targets distinct SH2-containing proteins. This leads to regulated augmentation of signal transduction activities involved in KS hyperplasia such as intracellular calcium mobilization, activation of NFAT and AP-1

transcription factors, and production of inflammatory cytokines and angiogenic growth factors (65). While the ITAM-containing sequence in RRV R1 is distributed over a longer stretch of cytoplasmic tail domain than seen in KSHV K1, both ITAM-bearing proteins utilize similar signal-inducing properties, mediate B cell activation events independent of traditional BCR engagement, and contribute to the oncogenic nature of these viruses (25).

Retroviruses have been found to encode ITAM-containing sequences within the subunits of viral envelope polyproteins. Bovine leukemia virus (BLV) is a B cell lymphotrophic retrovirus that causes chronic disease associated with non-neoplastic proliferation of B cells in cattle, and induces terminal B cell leukemia in sheep. The BLV envelope gene is initially synthesized as a 72 kDa glycoprotein (gp72) and is subsequently processed into a surface subunit (gp51) and a transmembrane subunit (gp30) (6, 105). While gp51 serves as a determinant of cellular tropism, gp30 serves to anchor the gp51-gp30 complex within both the plasma membrane and virions for mediation of virus-cell fusion. The C-terminal cytoplasmic tail of gp30 contains three $Y_{XX}L$ motifs, two of which together generate a functional ITAM. Studies using site-directed mutagenesis to create gp30 ITAMs containing tyrosine to alanine substitutions found that both tyrosines of the ITAM are important for BLV infection, propagation, and signal transduction (6, 105). Mouse mammary tumor virus (MMTV) is an additional oncogenic retrovirus containing an ITAM within its envelope protein. MMTV induces mammary carcinoma in mice and serves as a model for virus-induced cancer. In vivo, MMTV-induced transformation of mammary epithelial cells is partially mediated through proviral integration and insertional activation of cellular oncogenes, including members of the wnt and fibroblast growth factor (fgf) families (53, 93).

The MMTV envelope protein (Env) contains two subunits: a cell surface subunit (SU) and transmembrane subunit (TM). An ITAM within the SU domain was identified as a mediator of epithelial cell transformation during MMTV infection after it was demonstrated that ectopically expressed MMTV Env is sufficient for induction of transformation hallmarks in normal immortalized mammary epithelial cells. Further examination found that Env ITAM-mediated signaling utilizes Syk, and that mutation of critical tyrosine residues abrogates Env signaling, resulting in altered mammary epithelial cell transformation and attenuated tumorigenesis (93). Recent studies also demonstrate that the MMTV Env ITAM activates Src to mediate suppression of apoptosis in mammary epithelial cells. The investigation of mechanisms driving MMTV ITAM-mediated transformation of nonhematopoetic cells is important for the identification of novel modes of breast cancer induction and effective treatment of cancers in which ITAM-mediated signaling has been implicated (53).

Currently, there are two non-oncogenic viruses reported to encode ITAM containing proteins: hantavirus and simian immunodeficiency virus (SIV). Hantaviruses are enveloped negative-stranded RNA viruses belonging to the Bunyaviridae family. Hantaviruses infect human endothelial and immune cells, causing hemorrhagic fever with renal syndrome (HFRS) and hantavirus pulmonary syndrome (HPS) (38, 39). The hantavirus M genome segment encodes surface glycoproteins G1 and G2. Amino acid alignment of the G1 cytoplasmic tail of hantaviruses found that all HPS-causing viruses contain a conserved ITAM. The absence of this conserved motif in HFRS-causing and nonpathogenic hantavirus strains suggests an essential role for the ITAM-containing protein in hantavirus pathogenicity. The hantavirus G1 ITAM interacts with Src kinase Lyn, and Syk family

members Syk and Zap-70 to alter normal cell signaling responses and subsequently modulate immune and endothelial cell function. Conserved tyrosine residues within the cytoplasmic tail of G1 were also identified as determinants for polyubiquitination of the ITAM-bearing protein (38, 39). SIV, a primate lentivirus, induces a disease similar to human AIDS that is characterized by depletion of $CD4^+$ T cells, opportunistic infections, and subsequent death of infected animals. Investigation into the acute pathogenesis displayed by a particular SIV isolate highlighted a novel ability of the isolate to replicate within and induce proliferation of unstimulated PBMCs (32, 68). The primary pathogenic-determinant of this highly virulent isolate was identified to be an arginine to tyrosine mutation within the viral protein Nef. Tyrosine substitution generates an ITAM in the N-terminal anchor domain which was shown to be functional for activation of downstream ITAM-signaling intermediates including Lck and Zap-70. Finally, the Nef ITAM was found to be necessary and sufficient for Lck activation of NFAT, a key downstream intermediate of T cell activation (32, 68).

As a final note, an ITAM-like sequence has been identified in only one non-enveloped virus to date: coxsackievirus. However, substitution of critical tyrosine residues within the ITAM-like region of capsid protein VP2 attenuated the virus used in these studies, leaving interpretation of the results presented on ITAM function unclear (52). Coxsackievirus B3 (CVB3) is a single-stranded, positive sense RNA virus belonging to the family Picornaviridae and genus Enterovirus. CVB3 infection, while generally asymptomatic, can lead to myocarditis and inflammatory diseases associated with the pancreas and/or nervous system (52, 85). The 7.4kb genome encodes a single polyprotein. Following translation, viral proteases cleave the polyprotein into three fragments: P1, P2, and P3. The P1 fragment is

additionally cleaved to produce structural proteins VP0, VP1, and VP3. Autocleavage of VP0 generates VP2 and VP4. Finally, the P2 and P3 fragments are further modified to generate seven non-structural proteins (52, 85). In ITAM-like sequence was identified within the C-terminal region of VP2, and in an effort to identify a role for the putative ITAM, mutant CVB3 virus and protein constructs were generated in which VP2 tyrosines 240 and 254 were substituted with phenylalanine. VP2 was shown to be phosphorylated on tyrosine residues, and the ITAM-signaling intermediate Syk was found to be associated with wild-type CVB3 VP0, but not the tyrosine-to-phenylalanine mutant VP0-YYFF. Furthermore, wild-type CVB3 and ectopically expressed VP2 were able to activate NF-κB while the YYFF mutant was not, and interlukin-6 (IL-6) secretion was abrogated in CVB3-YYFF infected cells. While these data support CVB3 V2 ITAM function, viral titers corresponding to the infection time points used for these experiments show that CVB3-YYFF is severely attenuated (52). Therefore, the lack of tyrosine phosphorylation, Syk association, NF-κB activation, and IL-6 secretion observed with CVB3-YYFF could well be due to defective replication rather than defective ITAM function.

As discussed, viral ITAMs have been implicated in the mediation of a variety of viral and host cellular responses involving pathogenesis and oncogenesis. In Chapter 2, I will present studies investigating the role of a newly identified ITAM in determining the activation of essential cellular components and subsequent viral spread during reovirus infection.

REFERENCES

1. 1955. ENTERIC cytopathogenic human orphan (ECHO) viruses. Science **122:**1187-1188.

2. **Agosto, M. A., K. S. Myers, T. Ivanovic, and M. L. Nibert.** 2008. A positive-feedback mechanism promotes reovirus particle conversion to the intermediate associated with membrane penetration. Proceedings of the National Academy of Sciences of the United States of America **105:**10571-10576.

3. **Anafu, A. A., C. H. Bowen, C. R. Chin, A. L. Brass, and G. H. Holm.** 2013. Interferon-inducible Transmembrane Protein 3 (IFITM3) Restricts Reovirus Cell Entry. The Journal of biological chemistry **288:**17261-17271.

4. **Barton, E. S., J. L. Connolly, J. C. Forrest, J. D. Chappell, and T. S. Dermody.** 2001. Utilization of sialic acid as a coreceptor enhances reovirus attachment by multistep adhesion strengthening. The Journal of biological chemistry **276:**2200-2211.

5. **Barton, E. S., J. C. Forrest, J. L. Connolly, J. D. Chappell, Y. Liu, F. J. Schnell, A. Nusrat, C. A. Parkos, and T. S. Dermody.** 2001. Junction adhesion molecule is a receptor for reovirus. Cell **104:**441-451.

6. **Beaufils, P., D. Choquet, R. Z. Mamoun, and B. Malissen.** 1993. The (YXXL/I)2 signalling motif found in the cytoplasmic segments of the bovine leukaemia virus envelope protein and Epstein-Barr virus latent membrane protein 2A can elicit early and late lymphocyte activation events. The EMBO journal **12:**5105-5112.

7. **Bellamy, A. R., L. Shapiro, J. T. August, and W. K. Joklik.** 1967. Studies on reovirus RNA. I. Characterization of reovirus genome RNA. Journal of molecular biology **29:**1-17.

8. **Berger, A. K., and P. Danthi.** 2013. Reovirus activates a caspase-independent cell death pathway. mBio **4:**e00178-00113.

9. **Bisaillon, M., J. Bergeron, and G. Lemay.** 1997. Characterization of the nucleoside triphosphate phosphohydrolase and helicase activities of the reovirus lambda1 protein. The Journal of biological chemistry **272:**18298-18303.

10. **Boehme, K. W., M. Ikizler, T. Kobayashi, and T. S. Dermody.** 2011. Reverse genetics for mammalian reovirus. Methods **55:**109-113.

11. **Bradshaw, J. M.** 2010. The Src, Syk, and Tec family kinases: distinct types of molecular switches. Cellular signalling **22:**1175-1184.

12. **Brentano, L., D. L. Noah, E. G. Brown, and B. Sherry.** 1998. The reovirus protein mu2, encoded by the M1 gene, is an RNA-binding protein. Journal of virology **72:**8354-8357.

13. **Broering, T. J., J. S. Parker, P. L. Joyce, J. Kim, and M. L. Nibert.** 2002. Mammalian reovirus nonstructural protein microNS forms large inclusions and colocalizes with reovirus microtubule-associated protein micro2 in transfected cells. Journal of virology **76:**8285-8297.

14. **Burkhardt, A. L., J. B. Bolen, E. Kieff, and R. Longnecker.** 1992. An Epstein-Barr virus transformation-associated membrane protein interacts with src family tyrosine kinases. Journal of virology **66:**5161-5167.

15. **Burstin, S. J., D. R. Spriggs, and B. N. Fields.** 1982. Evidence for functional domains on the reovirus type 3 hemagglutinin. Virology **117:**146-155.

16. **Carvalho, J., M. M. Arnold, and M. L. Nibert.** 2007. Silencing and complementation of reovirus core protein mu2: functional correlations with mu2-microtubule association and differences between virus- and plasmid-derived mu2. Virology **364:**301-316.

17. **Chen, F. E., D. B. Huang, Y. Q. Chen, and G. Ghosh.** 1998. Crystal structure of p50/p65 heterodimer of transcription factor NF-kappaB bound to DNA. Nature **391:**410-413.

18. **Clarke, P., R. L. Debiasi, S. M. Meintzer, B. A. Robinson, and K. L. Tyler.** 2005. Inhibition of NF-kappa B activity and cFLIP expression contribute to viral-induced apoptosis. Apoptosis : an international journal on programmed cell death **10:**513-524.

19. **Clarke, P., S. M. Meintzer, S. Gibson, C. Widmann, T. P. Garrington, G. L. Johnson, and K. L. Tyler.** 2000. Reovirus-induced apoptosis is mediated by TRAIL. Journal of virology **74:**8135-8139.

20. **Clarke, P., S. M. Meintzer, L. A. Moffitt, and K. L. Tyler.** 2003. Two distinct phases of virus-induced nuclear factor kappa B regulation enhance tumor necrosis factor-related apoptosis-inducing ligand-mediated apoptosis in virus-infected cells. The Journal of biological chemistry **278:**18092-18100.

21. **Cleveland, D. R., H. Zarbl, and S. Millward.** 1986. Reovirus guanylyltransferase is L2 gene product lambda 2. Journal of virology **60:**307-311.

22. **Coffey, C. M., A. Sheh, I. S. Kim, K. Chandran, M. L. Nibert, and J. S. Parker.** 2006. Reovirus outer capsid protein micro1 induces apoptosis and associates with lipid droplets, endoplasmic reticulum, and mitochondria. Journal of virology **80:**8422-8438.

23. **Connolly, J. L., E. S. Barton, and T. S. Dermody.** 2001. Reovirus binding to cell surface sialic acid potentiates virus-induced apoptosis. Journal of virology **75:**4029-4039.

24. **Connolly, J. L., S. E. Rodgers, P. Clarke, D. W. Ballard, L. D. Kerr, K. L. Tyler, and T. S. Dermody.** 2000. Reovirus-induced apoptosis requires activation of transcription factor NF-kappaB. Journal of virology **74:**2981-2989.

25. **Damania, B., M. DeMaria, J. U. Jung, and R. C. Desrosiers.** 2000. Activation of lymphocyte signaling by the R1 protein of rhesus monkey rhadinovirus. Journal of virology **74:**2721-2730.

26. **Danthi, P.** 2011. Enter the kill zone: initiation of death signaling during virus entry. Virology **411:**316-324.

27. **Danthi, P., C. M. Coffey, J. S. Parker, T. W. Abel, and T. S. Dermody.** 2008. Independent regulation of reovirus membrane penetration and apoptosis by the mu1 phi domain. PLoS pathogens **4:**e1000248.

28. **Danthi, P., K. M. Guglielmi, E. Kirchner, B. Mainou, T. Stehle, and T. S. Dermody.** 2010. From touchdown to transcription: the reovirus cell entry pathway. Current topics in microbiology and immunology **343:**91-119.

29. **Danthi, P., M. W. Hansberger, J. A. Campbell, J. C. Forrest, and T. S. Dermody.** 2006. JAM-A-independent, antibody-mediated uptake of reovirus into cells leads to apoptosis. Journal of virology **80:**1261-1270.

30. **Danthi, P., T. Kobayashi, G. H. Holm, M. W. Hansberger, T. W. Abel, and T. S. Dermody.** 2008. Reovirus apoptosis and virulence are regulated by host cell membrane penetration efficiency. Journal of virology **82:**161-172.

31. **Danthi, P., A. J. Pruijssers, A. K. Berger, G. H. Holm, S. S. Zinkel, and T. S. Dermody.** 2010. Bid regulates the pathogenesis of neurotropic reovirus. PLoS pathogens **6:**e1000980.

32. **Dehghani, H., C. R. Brown, R. Plishka, A. Buckler-White, and V. M. Hirsch.** 2002. The ITAM in Nef influences acute pathogenesis of AIDS-inducing simian immunodeficiency viruses SIVsm and SIVagm without altering kinetics or extent of viremia. Journal of virology **76:**4379-4389.

33. **Dermody, T. S., J. Parker, B. Sherry.** 2013. Orthoreoviruses, p. 1304-1346. *In* D. M. K. a. P. M. Howley (ed.), Fields Virology, 6th ed, vol. 2. Wolters Kluwer Health/Lippincott Williams & Wilkins, Philadelphia.

34. **DiDonato, J. A., M. Hayakawa, D. M. Rothwarf, E. Zandi, and M. Karin.** 1997. A cytokine-responsive IkappaB kinase that activates the transcription factor NF-kappaB. Nature **388:**548-554.

35. **Ebert, D. H., J. Deussing, C. Peters, and T. S. Dermody.** 2002. Cathepsin L and cathepsin B mediate reovirus disassembly in murine fibroblast cells. The Journal of biological chemistry **277:**24609-24617.

36. **Farsetta, D. L., K. Chandran, and M. L. Nibert.** 2000. Transcriptional activities of reovirus RNA polymerase in recoated cores. Initiation and elongation are regulated by separate mechanisms. The Journal of biological chemistry **275:**39693-39701.

37. **Fotheringham, J. A., N. E. Coalson, and N. Raab-Traub.** 2012. Epstein-Barr virus latent membrane protein-2A induces ITAM/Syk- and Akt-dependent epithelial migration through alphav-integrin membrane translocation. Journal of virology **86:**10308-10320.

38. **Geimonen, E., I. Fernandez, I. N. Gavrilovskaya, and E. R. Mackow.** 2003. Tyrosine residues direct the ubiquitination and degradation of the NY-1 hantavirus G1 cytoplasmic tail. Journal of virology **77:**10760-10868.

39. **Geimonen, E., R. LaMonica, K. Springer, Y. Farooqui, I. N. Gavrilovskaya, and E. R. Mackow.** 2003. Hantavirus pulmonary syndrome-associated hantaviruses contain conserved and functional ITAM signaling elements. Journal of virology **77:**1638-1643.

40. **Hamerman, J. A., and L. L. Lanier.** 2006. Inhibition of immune responses by ITAM-bearing receptors. Science's STKE : signal transduction knowledge environment **2006:**re1.

41. **Hansberger, M. W., J. A. Campbell, P. Danthi, P. Arrate, K. N. Pennington, K. B. Marcu, D. W. Ballard, and T. S. Dermody.** 2007. IkappaB kinase subunits alpha and gamma are required for activation of NF-kappaB and induction of apoptosis by mammalian reovirus. Journal of virology **81:**1360-1371.

42. **Hara, H., C. Ishihara, A. Takeuchi, L. Xue, S. W. Morris, J. M. Penninger, H. Yoshida, and T. Saito.** 2008. Cell type-specific regulation of ITAM-mediated NF-kappaB activation by the adaptors, CARMA1 and CARD9. J Immunol **181:**918-930.

43. **Hayden, M. S., and S. Ghosh.** 2012. NF-kappaB, the first quarter-century: remarkable progress and outstanding questions. Genes & development **26:**203-234.

44. **Holm, G. H., J. Zurney, V. Tumilasci, S. Leveille, P. Danthi, J. Hiscott, B. Sherry, and T. S. Dermody.** 2007. Retinoic acid-inducible gene-I and interferon-beta promoter stimulator-1 augment proapoptotic responses following mammalian reovirus infection via interferon regulatory factor-3. The Journal of biological chemistry **282:**21953-21961.

45. **Humphrey, M. B., L. L. Lanier, and M. C. Nakamura.** 2005. Role of ITAM-containing adapter proteins and their receptors in the immune system and bone. Immunological reviews **208:**50-65.

46. **Huynh, L., L. Wang, C. Shi, K. H. Park-Min, and L. B. Ivashkiv.** 2012. ITAM-coupled receptors inhibit IFNAR signaling and alter macrophage responses to TLR4 and Listeria monocytogenes. J Immunol **188:**3447-3457.

47. **Irvin, S. C., J. Zurney, L. S. Ooms, J. D. Chappell, T. S. Dermody, and B. Sherry.** 2012. A single-amino-acid polymorphism in reovirus protein mu2 determines repression of interferon signaling and modulates myocarditis. Journal of virology **86:**2302-2311.

48. **Ivanovic, T., M. A. Agosto, K. Chandran, and M. L. Nibert.** 2007. A role for molecular chaperone Hsc70 in reovirus outer capsid disassembly. The Journal of biological chemistry **282:**12210-12219.

49. **Ivanovic, T., M. A. Agosto, L. Zhang, K. Chandran, S. C. Harrison, and M. L. Nibert.** 2008. Peptides released from reovirus outer capsid form membrane pores that recruit virus particles. The EMBO journal **27:**1289-1298.

50. **Ivashkiv, L. B.** 2009. Cross-regulation of signaling by ITAM-associated receptors. Nature immunology **10:**340-347.

51. **Iwakiri, D., T. Minamitani, and M. Samanta.** 2013. Epstein-Barr Virus Latent Membrane Protein 2A Contributes to Anoikis Resistance through ERK Activation. Journal of virology **87:**8227-8234.

52. **Kim, D. S., J. H. Park, J. Y. Kim, D. Kim, and J. H. Nam.** 2012. A mechanism of immunoreceptor tyrosine-based activation motif (ITAM)-like sequences in the capsid protein VP2 in viral growth and pathogenesis of Coxsackievirus B3. Virus genes **44:**176-182.

53. **Kim, H. H., S. M. Grande, J. G. Monroe, and S. R. Ross.** 2012. Mouse mammary tumor virus suppresses apoptosis of mammary epithelial cells through ITAM-mediated signaling. Journal of virology **86:**13232-13240.

54. **Kim, J., J. S. Parker, K. E. Murray, and M. L. Nibert.** 2004. Nucleoside and RNA triphosphatase activities of orthoreovirus transcriptase cofactor mu2. The Journal of biological chemistry **279:**4394-4403.

55. **Kirchner, E., K. M. Guglielmi, H. M. Strauss, T. S. Dermody, and T. Stehle.** 2008. Structure of reovirus sigma1 in complex with its receptor junctional adhesion molecule-A. PLoS pathogens **4:**e1000235.

56. **Knowlton, J. J., T. S. Dermody, and G. H. Holm.** 2012. Apoptosis induced by mammalian reovirus is beta interferon (IFN) independent and enhanced by IFN regulatory factor 3- and NF-kappaB-dependent expression of Noxa. Journal of virology **86:**1650-1660.

57. **Kobayashi, T., J. D. Chappell, P. Danthi, and T. S. Dermody.** 2006. Gene-specific inhibition of reovirus replication by RNA interference. Journal of virology **80:**9053-9063.

58. **Kobayashi, T., L. S. Ooms, J. D. Chappell, and T. S. Dermody.** 2009. Identification of functional domains in reovirus replication proteins muNS and mu2. Journal of virology **83:**2892-2906.

59. **Kobayashi, T., L. S. Ooms, M. Ikizler, J. D. Chappell, and T. S. Dermody.** 2010. An improved reverse genetics system for mammalian orthoreoviruses. Virology **398:**194-200.

60. **Kominsky, D. J., R. J. Bickel, and K. L. Tyler.** 2002. Reovirus-induced apoptosis requires both death receptor- and mitochondrial-mediated caspase-dependent pathways of cell death. Cell death and differentiation **9:**926-933.

61. **Lagunoff, M., D. M. Lukac, and D. Ganem.** 2001. Immunoreceptor tyrosine-based activation motif-dependent signaling by Kaposi's sarcoma-associated herpesvirus K1 protein: effects on lytic viral replication. Journal of virology **75:**5891-5898.

62. **Lagunoff, M., R. Majeti, A. Weiss, and D. Ganem.** 1999. Deregulated signal transduction by the K1 gene product of Kaposi's sarcoma-associated herpesvirus. Proceedings of the National Academy of Sciences of the United States of America **96:**5704-5709.

63. **Lanier, L. L.** 2006. Viral immunoreceptor tyrosine-based activation motif (ITAM)-mediated signaling in cell transformation and cancer. Trends in cell biology **16:**388-390.

64. **Lanier, L. L., and A. B. Bakker.** 2000. The ITAM-bearing transmembrane adaptor DAP12 in lymphoid and myeloid cell function. Immunology today **21:**611-614.

65. **Lee, B. S., S. H. Lee, P. Feng, H. Chang, N. H. Cho, and J. U. Jung.** 2005. Characterization of the Kaposi's sarcoma-associated herpesvirus K1 signalosome. Journal of virology **79:**12173-12184.

66. **Lee, H., J. Guo, M. Li, J. K. Choi, M. DeMaria, M. Rosenzweig, and J. U. Jung.** 1998. Identification of an immunoreceptor tyrosine-based activation motif of K1 transforming protein of Kaposi's sarcoma-associated herpesvirus. Molecular and cellular biology **18:**5219-5228.

67. **Lu, J., W. H. Lin, S. Y. Chen, R. Longnecker, S. C. Tsai, C. L. Chen, and C. H. Tsai.** 2006. Syk tyrosine kinase mediates Epstein-Barr virus latent membrane protein 2A-induced cell migration in epithelial cells. The Journal of biological chemistry **281:**8806-8814.

68. **Luo, W., and B. M. Peterlin.** 1997. Activation of the T-cell receptor signaling pathway by Nef from an aggressive strain of simian immunodeficiency virus. Journal of virology **71:**9531-9537.

69. **Maginnis, M. S., J. C. Forrest, S. A. Kopecky-Bromberg, S. K. Dickeson, S. A. Santoro, M. M. Zutter, G. R. Nemerow, J. M. Bergelson, and T. S. Dermody.** 2006. Beta1 integrin mediates internalization of mammalian reovirus. Journal of virology **80:**2760-2770.

70. **Maginnis, M. S., B. A. Mainou, A. Derdowski, E. M. Johnson, R. Zent, and T. S. Dermody.** 2008. NPXY motifs in the beta1 integrin cytoplasmic tail are required for functional reovirus entry. Journal of virology **82:**3181-3191.

71. **Mainou, B. A., and T. S. Dermody.** 2011. Src kinase mediates productive endocytic sorting of reovirus during cell entry. Journal of virology **85:**3203-3213.

72. **Mainou, B. A., and T. S. Dermody.** 2012. Transport to late endosomes is required for efficient reovirus infection. Journal of virology **86:**8346-8358.

73. **Mainou, B. A., P. F. Zamora, A. W. Ashbrook, D. C. Dorset, K. S. Kim, and T. S. Dermody.** 2013. Reovirus cell entry requires functional microtubules. mBio **4**.

74. **Matoba, Y., W. S. Colucci, B. N. Fields, and T. W. Smith.** 1993. The reovirus M1 gene determines the relative capacity of growth of reovirus in cultured bovine aortic endothelial cells. The Journal of clinical investigation **92:**2883-2888.

75. **Matoba, Y., B. Sherry, B. N. Fields, and T. W. Smith.** 1991. Identification of the viral genes responsible for growth of strains of reovirus in cultured mouse heart cells. The Journal of clinical investigation **87:**1628-1633.

76. **Mbisa, J. L., M. M. Becker, S. Zou, T. S. Dermody, and E. G. Brown.** 2000. Reovirus mu2 protein determines strain-specific differences in the rate of viral inclusion formation in L929 cells. Virology **272:**16-26.

77. **Miller, C. L., M. M. Arnold, T. J. Broering, C. E. Hastings, and M. L. Nibert.** 2010. Localization of mammalian orthoreovirus proteins to cytoplasmic factory-like structures via nonoverlapping regions of microNS. Journal of virology **84:**867-882.

78. **Miller, C. L., T. J. Broering, J. S. Parker, M. M. Arnold, and M. L. Nibert.** 2003. Reovirus sigma NS protein localizes to inclusions through an association requiring the mu NS amino terminus. Journal of virology **77:**4566-4576.

79. **Miller, C. L., J. S. Parker, J. B. Dinoso, C. D. Piggott, M. J. Perron, and M. L. Nibert.** 2004. Increased ubiquitination and other covariant phenotypes attributed to a strain- and temperature-dependent defect of reovirus core protein mu2. Journal of virology **78:**10291-10302.

80. **Mocsai, A., J. Ruland, and V. L. Tybulewicz.** 2010. The SYK tyrosine kinase: a crucial player in diverse biological functions. Nature reviews. Immunology **10:**387-402.

81. **Noble, S., and M. L. Nibert.** 1997. Core protein mu2 is a second determinant of nucleoside triphosphatase activities by reovirus cores. Journal of virology **71:**7728-7735.

82. **O'Donnell, S. M., M. W. Hansberger, J. L. Connolly, J. D. Chappell, M. J. Watson, J. M. Pierce, J. D. Wetzel, W. Han, E. S. Barton, J. C. Forrest, T. Valyi-Nagy, F. E. Yull, T. S. Blackwell, J. N. Rottman, B. Sherry, and T. S. Dermody.** 2005. Organ-specific roles for transcription factor NF-kappaB in reovirus-induced apoptosis and disease. The Journal of clinical investigation **115:**2341-2350.

83. **Ooms, L. S., W. G. Jerome, T. S. Dermody, and J. D. Chappell.** 2012. Reovirus replication protein mu2 influences cell tropism by promoting particle assembly within viral inclusions. Journal of virology **86:**10979-10987.

84. **Ooms, L. S., T. Kobayashi, T. S. Dermody, and J. D. Chappell.** 2010. A post-entry step in the mammalian orthoreovirus replication cycle is a determinant of cell tropism. The Journal of biological chemistry **285:**41604-41613.

85. **Pallansch, M., and R. Raymond.** 2007. Enteroviruses: Polioviruses, Coxsackieviruses, Echoviruses, and Newer Enteroviruses, p. 839-893. *In* D. M. K. a. P. M. Howley (ed.), Fields Virology, 5th ed, vol. 1. Wolters Kluwer Health/Lippincott Williams & Wilkins, Philadelphia.

86. **Parker, J. S., T. J. Broering, J. Kim, D. E. Higgins, and M. L. Nibert.** 2002. Reovirus core protein mu2 determines the filamentous morphology of viral inclusion bodies by interacting with and stabilizing microtubules. Journal of virology **76:**4483-4496.

87. **Philpott, N., T. Bakken, C. Pennell, L. Chen, J. Wu, and M. Cannon.** 2011. The Kaposi's sarcoma-associated herpesvirus G protein-coupled receptor contains an immunoreceptor tyrosine-based inhibitory motif that activates Shp2. Journal of virology **85:**1140-1144.

88. **Rahman, M. M., and G. McFadden.** 2011. Modulation of NF-kappaB signalling by microbial pathogens. Nature reviews. Microbiology **9:**291-306.

89. **Ramos-Alvarez, M., and A. B. Sabin.** 1958. Enteropathogenic viruses and bacteria; role in summer diarrheal diseases of infancy and early childhood. Journal of the American Medical Association **167:**147-156.

90. **Reinisch, K. M., M. L. Nibert, and S. C. Harrison.** 2000. Structure of the reovirus core at 3.6 A resolution. Nature **404:**960-967.

91. **Reiter, D. M., J. M. Frierson, E. E. Halvorson, T. Kobayashi, T. S. Dermody, and T. Stehle.** 2011. Crystal structure of reovirus attachment protein sigma1 in complex with sialylated oligosaccharides. PLoS pathogens **7:**e1002166.

92. **Rosen, L., J. F. Hovis, F. M. Mastrota, J. A. Bell, and R. J. Huebner.** 1960. Observations on a newly recognized virus (Abney) of the reovirus family. American journal of hygiene **71:**258-265.

93. **Ross, S. R., J. W. Schmidt, E. Katz, L. Cappelli, S. Hultine, P. Gimotty, and J. G. Monroe.** 2006. An immunoreceptor tyrosine activation motif in the mouse mammary tumor virus envelope protein plays a role in virus-induced mammary tumors. Journal of virology **80:**9000-9008.

94. **Sada, K., T. Takano, S. Yanagi, and H. Yamamura.** 2001. Structure and function of Syk protein-tyrosine kinase. Journal of biochemistry **130:**177-186.

95. **Scholle, F., R. Longnecker, and N. Raab-Traub.** 1999. Epithelial cell adhesion to extracellular matrix proteins induces tyrosine phosphorylation of the Epstein-Barr virus latent membrane protein 2: a role for C-terminal Src kinase. Journal of virology **73:**4767-4775.

96. **Shatkin, A. J., and J. D. Sipe.** 1968. Single-stranded, adenine-rich RNA from purified reoviruses. Proceedings of the National Academy of Sciences of the United States of America **59:**246-253.

97. **Shatkin, A. J., J. D. Sipe, and P. Loh.** 1968. Separation of ten reovirus genome segments by polyacrylamide gel electrophoresis. Journal of virology **2:**986-991.

98. **Sherry, B.** 2009. Rotavirus and reovirus modulation of the interferon response. Journal of interferon & cytokine research : the official journal of the International Society for Interferon and Cytokine Research **29:**559-567.

99. **Starnes, M. C., and W. K. Joklik.** 1993. Reovirus protein lambda 3 is a poly(C)-dependent poly(G) polymerase. Virology **193:**356-366.

100. **Sturzenbecker, L. J., M. Nibert, D. Furlong, and B. N. Fields.** 1987. Intracellular digestion of reovirus particles requires a low pH and is an essential step in the viral infectious cycle. Journal of virology **61:**2351-2361.

101. **Tassiulas, I., X. Hu, H. Ho, Y. Kashyap, P. Paik, Y. Hu, C. A. Lowell, and L. B. Ivashkiv.** 2004. Amplification of IFN-alpha-induced STAT1 activation and inflammatory function by Syk and ITAM-containing adaptors. Nature immunology **5:**1181-1189.

102. **Tsang, E., A. M. Giannetti, D. Shaw, M. Dinh, J. K. Tse, S. Gandhi, H. Ho, S. Wang, E. Papp, and J. M. Bradshaw.** 2008. Molecular mechanism of the Syk activation switch. The Journal of biological chemistry **283:**32650-32659.

103. **Tyler, K. L., M. K. Squier, S. E. Rodgers, B. E. Schneider, S. M. Oberhaus, T. A. Grdina, J. J. Cohen, and T. S. Dermody.** 1995. Differences in the capacity of reovirus strains to induce apoptosis are determined by the viral attachment protein sigma 1. Journal of virology **69:**6972-6979.

104. **Underhill, D. M., and H. S. Goodridge.** 2007. The many faces of ITAMs. Trends in immunology **28:**66-73.

105. **Willems, F., F. Andris, D. Xu, D. Abramowicz, M. Wissing, M. Goldman, and O. Leo.** 1995. The induction of human T cell unresponsiveness by soluble anti-CD3 mAb requires T cell activation. International immunology **7:**1593-1598.

106. **Wisniewski, M. L., B. G. Werner, L. G. Hom, L. J. Anguish, C. M. Coffey, and J. S. Parker.** 2011. Reovirus infection or ectopic expression of outer capsid protein micro1 induces apoptosis independently of the cellular proapoptotic proteins Bax and Bak. Journal of virology **85:**296-304.

107. **Yin, P., M. Cheang, and K. M. Coombs.** 1996. The M1 gene is associated with differences in the temperature optimum of the transcriptase activity in reovirus core particles. Journal of virology **70:**1223-1227.

108. **Yin, P., N. D. Keirstead, T. J. Broering, M. M. Arnold, J. S. Parker, M. L. Nibert, and K. M. Coombs.** 2004. Comparisons of the M1 genome segments and encoded mu2 proteins of different reovirus isolates. Virology journal **1:**6.

109. **Zandi, E., D. M. Rothwarf, M. Delhase, M. Hayakawa, and M. Karin.** 1997. The IkappaB kinase complex (IKK) contains two kinase subunits, IKKalpha and IKKbeta, necessary for IkappaB phosphorylation and NF-kappaB activation. Cell **91:**243-252.

110. **Zhang, X., S. B. Walker, P. R. Chipman, M. L. Nibert, and T. S. Baker.** 2003. Reovirus polymerase lambda 3 localized by cryo-electron microscopy of virions at a resolution of 7.6 A. Nature structural biology **10:**1011-1018.

111. **Zou, S., and E. G. Brown.** 1992. Nucleotide sequence comparison of the M1 genome segment of reovirus type 1 Lang and type 3 Dearing. Virus research **22:**159-164.

112. **Zurney, J., T. Kobayashi, G. H. Holm, T. S. Dermody, and B. Sherry.** 2009. Reovirus mu2 protein inhibits interferon signaling through a novel mechanism involving nuclear accumulation of interferon regulatory factor 9. Journal of virology **83:**2178-2187.

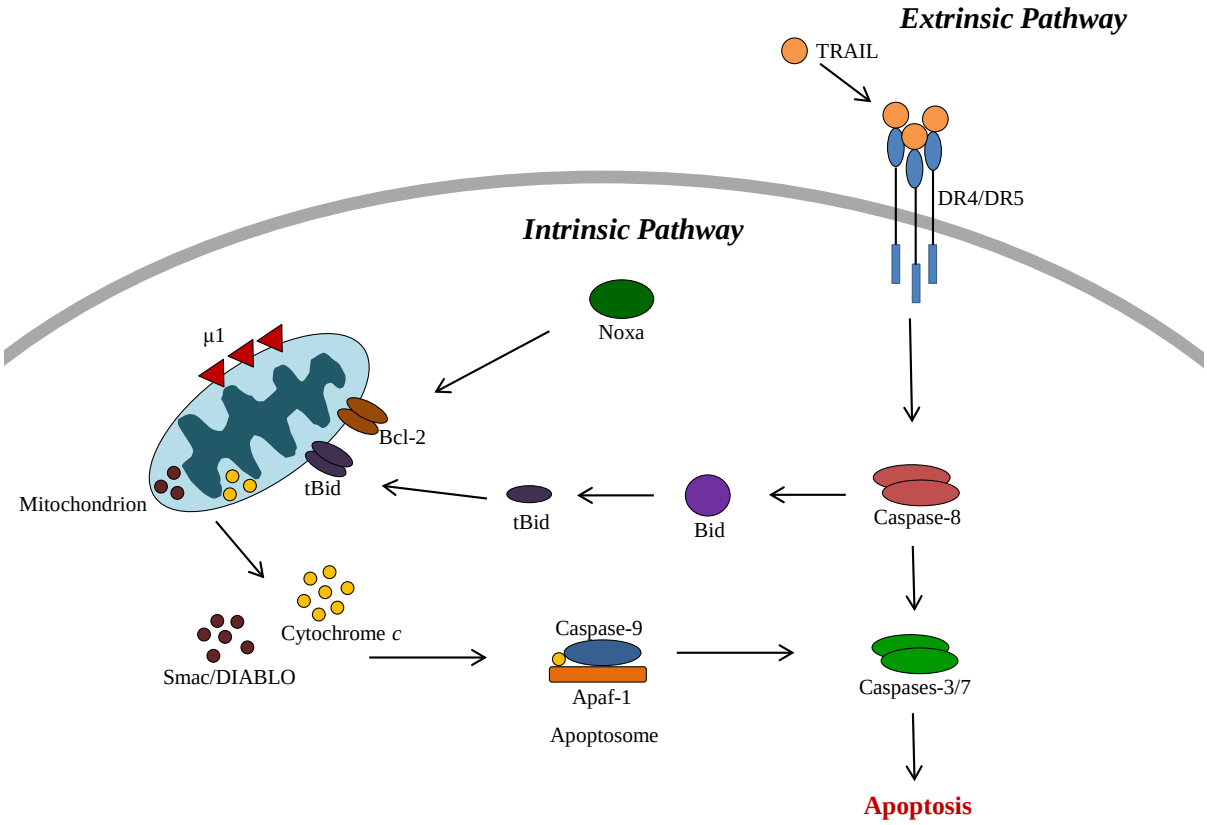

Figure 1.1. Reovirus infection induces apoptosis through both the intrinsic and extrinsic pathways. Reovirus induces release of tumor necrosis factor (TNF)-related apoptosis-inducing ligand (TRAIL) and upregulation of TRAIL-associated death receptors (DRs) DR4 and DR5 (19). DR activation is followed by activation of caspase-8 and subsequent cleavage of the pro-apoptotic Bcl-2 family member, Bid, into its truncated form, tBid (60). tBid translocates to the mitochondria and triggers the release of cytochrome c for apoptosome formation and activation of effector caspases, linking the extrinsic apoptotic pathway and the mitochondrial amplification loop of the intrinsic pathway (31). Reovirus infection also upregulates the proapoptotic BH3-only protein NOXA, which induces apoptosis through intrinsic pathway signaling intermediates (56). μ1 has been identified as the principal viral factor for stimulation of cellular apoptotic machinery (22, 27, 29). Ectopic expression of μ1 stimulates the release of cytochrome c and Smac/DIABLO into the cytosol, and the activation of both caspases 8 and 9 (106). While many other cell proteins, such as Bax and Bak, can participate in apoptosis, the pathway in this figure has been simplified to indicate only those factors known to participate in reovirus-induced apoptosis.

Figure adapted from P. Danthi (26).

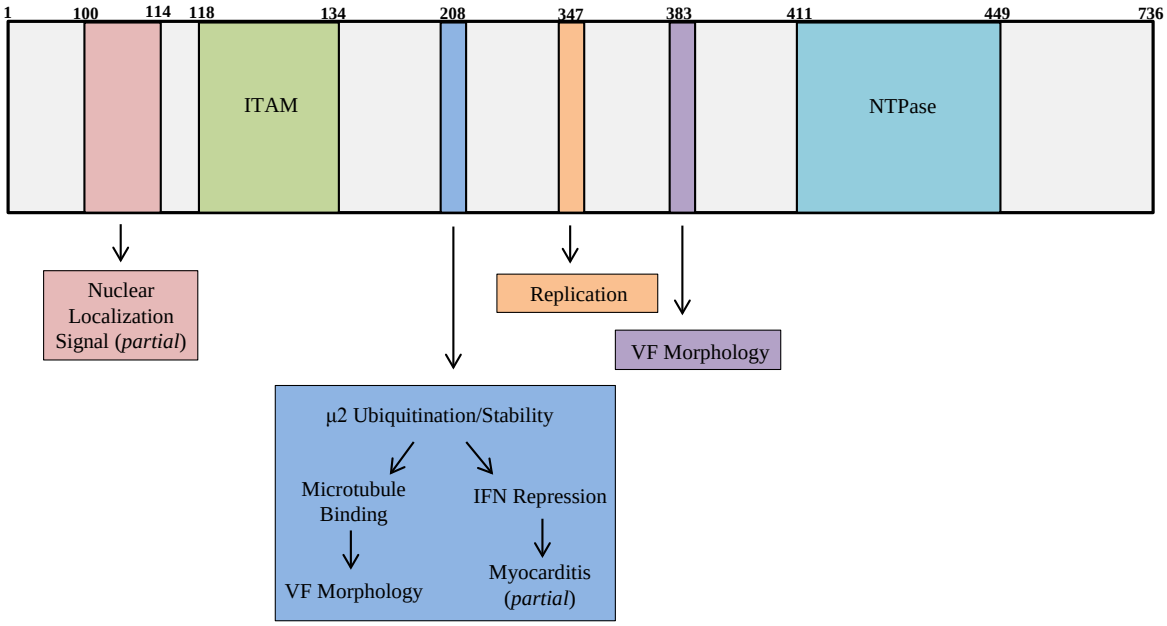

Figure 1.2. Reovirus protein μ2, encoded by the M1 gene segment. The μ2 protein contains nuclear localization signal that is critical for viral replication, suggesting that nuclear targeting of μ2 is a required step in reovirus infection (58). We have recently identified an immunoreceptor tyrosine-based activation motif (ITAM) containing the canonical motif YxxI/Lx_{6-12}YxxI/L. Amino acid 208 has been linked to strain-specific differences in μ2 uniquitination and stability, microtubule binding, viral factory (VF) morphology, interferon (IFN) repression, and induction of reovirus-induced myocarditis (47, 79, 86). Amino acid 347 has been identified as a determinant of strain-dependent replication efficiency in Madin-Darby canine kidney (MDCK) cells (83). Amino acid 383 has been identified as an additional determinant of VF morphology (58). An NTPase domain containing Walker A- and B-like motifs has been identified in the amino-terminal region of the M1 gene segment and is critical for viral replication (58).

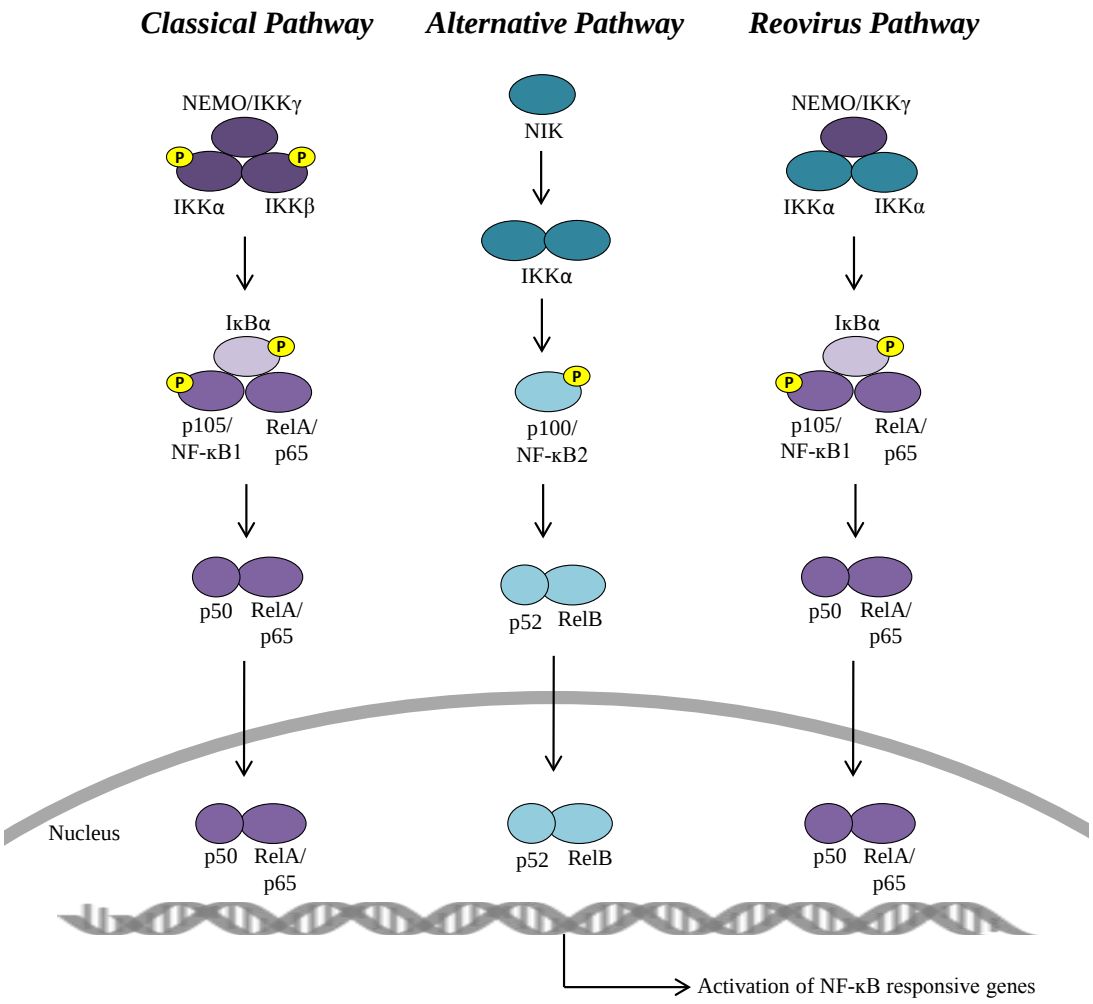

Figure 1.3. Reovirus NF-κB activation requires components of both the classical and alternative NF-κB signaling pathways. In the classical pathway, cell stimulation triggers activation of IKKβ. IKKβ associates with IKKα and the IKKβ regulatory protein NEMO/IKKγ. Subsequent phosphorylation of IκBα and p105/NF-κB1 results in IκBα degradation and cleavage of p105/NF-κB1 to form the NF-κB subunit p50. In the alternative pathway, stimulation induces NF-κB inducing kinase (NIK) activation of IKKα, resulting in phosphorylation and cleavage of p100/NF-κB2 to form the NF-κB subunit p52. NF-κB subunits p50 and p52 associate with NF-κB subunits RelA/p65 and RelB, respectively, and translocate to the nucleus (43, 88, 109). Reovirus infection triggers NF-κB activation through a novel mechanism involving IKKα and NEMO/IKKγ, but not IKKβ or NIK, which results in in IκBα proteolytic degradation, and nuclear translocation of NF-κB complexes containing p50 and RelA/p65 subunits (41).

Figure adapted from M. Rahman and G. McFadden (88).

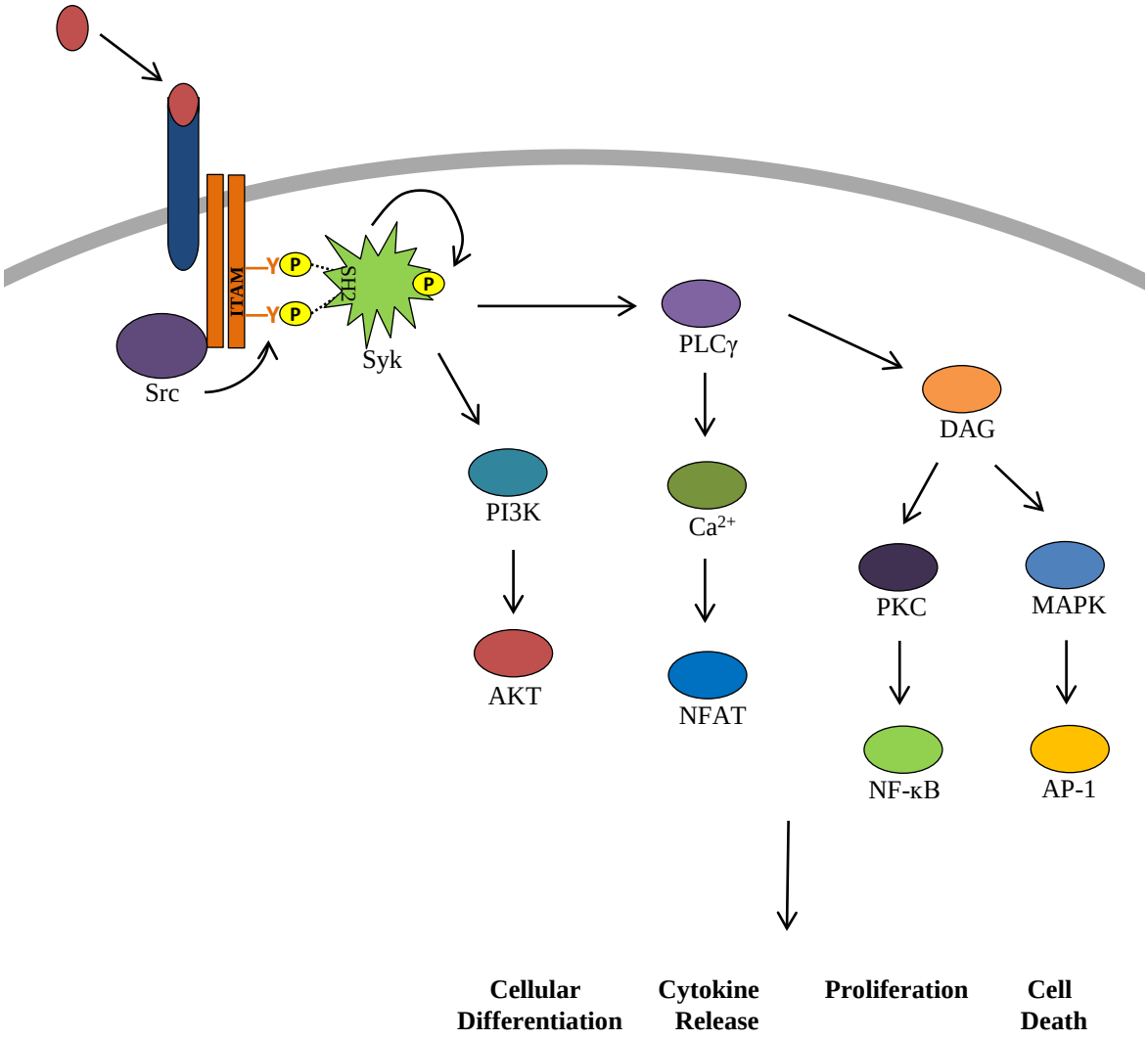

Figure 1.4. ITAM-mediated cellular signaling. Engagement of ITAM-associated receptors leads to phosphorylation of ITAM tyrosine residues by Src family kinases, resulting in recruitment of Syk tyrosine kinase. Interaction of Syk SH2 domains with ITAM phosphotyrosines stimulates Syk autophosphorylation and initiates downstream signaling cascades that result in a variety of cellular responses (80, 94, 102, 104). Effector molecules and transcription factors of importance activated during or in response to ITAM-mediated signaling include phosphatidylinositide 3-kinase (PI3K), protein kinase B (AKT), phospholipase-Cγ (PLCγ), nuclear factor of activated T cells (NFAT), diacylglycerol (DAG), protein kinase C (PKC), NF-κB, mitogen-activated protein kinases (MAPKs), and activator protein 1 (AP-1) (42, 50).

Figure adapted from L. Lanier (63).

CHAPTER 2

An ITAM in a Non-enveloped Virus Regulates Activation of NF-κB, Induction of Interferon-β, and Viral Spread

Rachael E. Stebbing[1*], Susan C. Irvin[1*], Efraín E. Rivera Serrano[1], Karl W. Boehme[2], Mine Ikizler[2], Jeffrey A. Yoder[1], Terence S. Dermody[2], and Barbara Sherry[1]

[1] Department of Molecular Biomedical Sciences and Center for Comparative Medicine and Translational Research, North Carolina State University, Raleigh NC 27607; [2] Departments of Pediatrics and [3]Pathology, Microbiology, and Immunology and [4] Elizabeth B. Lamb Center for Pediatric Research, Vanderbilt University School of Medicine, Nashville, TN 37232, USA

My contribution to this work: Figure 2, Figure 4, Figure 5, and manuscript text

[*]Manuscript to be submitted to Journal of Virology, with a statement that R. E. Stebbing and S. C. Irvin contributed equally.

ABSTRACT

Immunoreceptor tyrosine-based activation motifs (ITAMs) are signaling domains located within the cytoplasmic tails of many transmembrane receptors and associated adaptor proteins that mediate immune cell activation. ITAMs also have been identified in the cytoplasmic tails of some enveloped virus glycoproteins and play critical roles in viral pathogenesis and oncogenesis. Here, we identified ITAM sequences in three mammalian reovirus proteins: μ2, σ2, and λ2. We demonstrate for the first time that μ2 is phosphorylated, contains a functional ITAM, and activates NF-κB. Specifically, μ2 recruits the ITAM-signaling intermediate Syk to cytoplasmic viral factories and the μ2 ITAM is required for this translocation. Moreover, both the μ2 ITAM and Syk are required for maximal μ2 activation of NF-κB. A mutated virus lacking the μ2 ITAM activates less NF-κB and induces less of the downstream antiviral cytokine interferon (IFN)-β than wild type virus does despite similar replication. Notably, the consequences of these μ2 ITAM effects are cell type-specific. In non-specialized L929 cells where NF-κB is required for reovirus-induced apoptosis, the μ2 ITAM is advantageous for viral spread and enhances viral fitness. Conversely, in cardiac myocytes where the IFN response is critical for antiviral protection and NF-κB is not required for apoptosis, the μ2 ITAM stimulates cellular defense mechanisms and thereby diminishes viral fitness. These results suggest that the cell type-specific impact of the μ2 ITAM on viral spread likely reflects the cell type-specific functions of NF-κB and IFN-β. This first evidence for a functional ITAM in a non-enveloped virus

presents a novel mechanism for viral ITAM-mediated signaling with likely organ-specific consequences in the host.

INTRODUCTION

Immunoreceptor tyrosine-based activation motifs (ITAMs) are characterized by two critical tyrosine (Y) residues within the canonical motif YxxI/Lx_{6-12}YxxI/L. Often found in multiples, ITAMs are classically located within the cytoplasmic tail of transmembrane receptors and within the subunits of multi-component receptor complexes (32, 51). ITAMs are widely expressed throughout the immune system where they mediate activation of intracellular signaling by key immunoreceptors including T cell receptors (TCRs), B cell receptors (BCRs), and Fc receptors (FcRs). In myeloid and natural killer (NK) cells, this highly conserved motif has been identified in adaptor proteins DNAX-activating protein (DAP12) and Fc receptor-associated γ chain (FcRγ) (21, 32).

Engagement of ITAM-associated receptors leads to phosphorylation of ITAM tyrosine residues by Src family kinases and subsequent recruitment of spleen tyrosine kinase (Syk). Interaction of Syk SH2 domains with ITAM phosphotyrosines stimulates Syk autophosphorylation and activation, initiating downstream signaling cascades where effector molecules and transcription factors including PI3K, MAPKs, NFAT, and NF-κB stimulate an array of cellular responses involved in differentiation, cytokine release, proliferation, and survival (18, 23, 40, 51).

Interestingly, numerous enveloped viruses including hantavirus, Epstein-Barr virus (EBV), and Kaposi's sarcoma-associated herpesvirus (KSHV) encode ITAM-containing sequences within their genomes that participate in viral pathogenesis and oncogenesis through mediation of traditional cellular ITAM signaling intermediates (17, 32, 34, 44). To date, an ITAM-like sequence has been identified in only one non-enveloped virus, coxsackievirus, however evidence for ITAM function in that virus remains ambiguous (26).

Mammalian orthoreoviruses, commonly referred to as reoviruses, are nonenveloped double-stranded RNA (dsRNA) viruses belonging to the Reoviridae family. Reoviruses serve as highly tractable experimental models for studies of viral replication, pathogenesis, and virus-host interactions. Following infection of neonatal mice, reoviruses disseminate systemically, inducing strain-specific pathology in a variety of organs including the heart, central nervous system, and liver (10).

In primary murine cardiac myocytes, the capacity to induce myocarditis correlates with virus strain-specific differences in induction of and sensitivity to the antiviral cytokine interferon-β (IFN-β). Concordantly, nonmyocarditic reovirus strains induce cardiac lesions when the IFN response is disrupted (19, 41, 48). The reovirus M1 gene, which encodes minor core protein μ2, is the primary determinant of reovirus myocarditic potential (46, 47). Recently, sequence polymorphisms at μ2 amino acid 208 were found to be both required and sufficient for strain-specific differences in repression of IFN-β signaling, and μ2 amino acid 208 was identified as a determinant of the IFN-β response, viral spread and damage in cardiac myocytes, and myocarditis in neonatal mice (22). This μ2-mediated repression of IFN signaling is accompanied by accumulation of interferon regulatory factor 9 (IRF9) in the

nuclear fraction (55). Differences in induction of and sensitivity to IFN-β also segregate with the S2 and L2 genes, which encode the σ2, and λ2 proteins, respectively (48).

Reoviruses induce IFN by activating RIG-I-like pathogen recognition receptors (20, 25, 35). Following receptor engagement, signaling through the adaptor protein MAVS (also known as IPS-1, VISA, and Cardif) leads to activation of IFN transcription factors IRF3 and NF-κB. NF-κB mediates reovirus-induced apoptosis and subsequent pathogenesis in an organ/cell type-specific manner by either enhancing or preventing cell death signaling (19, 41). While reovirus activation of IRF3 is dependent on MAVS, NF-κB activation does not require this signaling intermediate (20). Reovirus protein μ1 is sufficient for induction of apoptosis when ectopically expressed, suggesting μ1 plays a role in reovirus-induced NF-κB activation (6). Additional mechanisms of reovirus-induced NF-κB activation have yet to be defined.

In this study, we found that minor core protein μ2 in reovirus strain type 3 Dearing (T3D) contains a functional ITAM that signals through Syk and regulates the activation of NF-κB and induction of IFN-β in a cell type specific manner. In L929 cells, where NF-κB is required for reovirus-mediated apoptosis, the μ2 ITAM is advantageous for viral spread, while in cardiac myocytes, where IFN-β is critical for protection against reovirus replication and cytopathic effects, the μ2 ITAM stimulates cellular defense mechanisms(41). These results suggest the μ2 ITAM has a cell type-specific role in reovirus replication and cytopathology, and provide evidence of a novel mechanism for ITAM-mediated signaling by a nonenveloped virus.

MATERIALS and METHODS

Cell lines. Mouse L929 cells were maintained in minimal essential medium (MEM) (SAFC Biosciences) supplemented with 5% fetal calf serum (FCS) (Atlanta Biologicals) and 2 mM L-glutamine (Mediatech). L929 cells were plated at 1.25 x 10^4 cells per well in 96-well clusters or at 5 x 10^5 cells per well in 24-well clusters. Cells were allowed to adhere 3 hours (h) prior to infection or transfection. HEK-293 cells (ATCC, CRL-1573) and AD-293 cells (Agilent Technologies), a derivative of HEK-293 cells with improved adherence, were maintained in Dulbecco's MEM (DMEM) (Gibco) supplemented with 10% FCS, and 110 mg/L sodium pyruvate (Mediatech). AD-293 cells were plated at 1.875 x 10^4 cells per well in 96-well clusters or at 4 x 10^5 cells per well in 6-well clusters. HEK-293 cells were plated at 3.5 x 10^4 cells per well in 96-well clusters or at 4 x 10^5 cells per well in 6-well clusters. HEK-293 and AD-293 cells were allowed to adhere at least 3 h prior to transfection or overnight before infection. Vero cells (ATCC, CCL-81) were maintained in DMEM (Gibco) supplemented with 10% FCS. Vero cells were plated at 5 x 10^4 cells per well in 8-well collagen-coated chamber slides (BD BioSciences) on the day before transfection.

Primary cardiac myocyte cultures. Timed-pregnant Cr:NIH(S) mice from the National Cancer Institute were maintained as a colony in a facility accredited by the Association for Assessment and Accreditation of Laboratory Animal Care. All animal procedures were approved by the North Carolina State University Institutional Animal Care and Use Committee. Primary cardiac myocyte cultures were generated from 1-day-old neonatal or term fetal Cr:NIH(S) mice resulting from timed pregnancies. Neonatal or term

fetal mice were euthanized, and the apical two-thirds of hearts were excised and trypsinized (1). To separate cardiac myocytes from rapidly adherent cardiac fibroblasts, cells were plated at 1.25 x 10^5 cells per well in 6-well clusters and incubated for 2 h at 37°C. Cardiac myocytes were resuspended in DMEM (Gibco) supplemented with 7% FCS (Atlanta Biologicals), 0.06% thymidine (Sigma-Aldrich), and 10 μg per ml of gentamicin (Sigma-Aldrich). Myocyte cultures contained ≤ 5% contamination with fibroblasts and were never passaged prior to use (54). Myocyte cultures were plated at 1.5 x 10^5 cells per well in 96-well clusters or 5 x 10^5 cells per well in 48-well clusters, and incubated for 2 days prior to infection.

Viruses. Wild-type reovirus strain T3D and mutant recombinant viruses were generated using plasmid-based reverse genetics (28). Tyrosine-to-phenylalanine mutations in the ITAMs were introduced into plasmids containing the T3D S2, M1, or L2 genes (28, 55) using the QuikChange Site-Directed Mutagenesis Kit (Agilent Technologies) according to the manufacturer's instructions with the following primers:

σ2 Y130F forward 5'-GTACGACTGCGATGATTTTCCATTTCTAGCGCGTG-3'
and reverse 5'-CACGCGCTAGAAATGGAAAATCATCGCAGTCGTAC-3';

σ2 Y144F forward 5'-GATTCAAACATCGGGTGTTTCAGCAATTGAGTGCTGTAAC-3'
and reverse 5'-GTTACAGCACTCAATTGCTGAAACACCCGATGTTTGAATC-3';

μ2 Y118F forward 5'-CTCAGGAAAGATGATGAATTCAATCAGCTAGCGCGTGC-3'
and reverse 5'-GCACGCGCTAGCTGATTGAATTCATCATCTTTCCTGAG-3';

μ2 Y131F forward 5'-CAAGATATCGGATGTCTTCGCACCTCTCATCTCATCC-3'
and reverse 5'-GGATGAGATGAGAGGTGCGAAGACATCCGATATCTTG-3';

λ2 Y671F forward 5'-CTTGGACATCTGGAGTGTTCTTCTTCTTGGTGGACC-3'

and reverse 5'-GGTCCACCAAGAAGAAGAACACTCCAGATGTCCAAG-3'; λ2 Y681F forward 5'GGTGGACCATTTTTATCGTTTTGAGACTTTATCTACGATCTCACG-3' and reverse 5'-CGTGAGATCGTAGATAAAGTCTCAAAACGATAAAAATGGTCCACC-3'. Monolayers of BHK-T7 cells at 90% confluency (3×10^6 cells) seeded in 60-mm dishes were co-transfected with plasmids representing the cloned reovirus genome using 3 μl of TransIT-LT1 transfection reagent (Mirus) per μg of plasmid DNA (29). Following 1–5 days of incubation, recombinant virus was isolated from transfected cells by plaque purification using monolayers of L929 cells. To confirm sequences of the mutant viruses, viral RNA was extracted from purified virions, subjected to Onestep RT-PCR (Qiagen) using gene-specific primers (sequences available upon request), and sequenced. Recombinant viruses were plaque purified, amplified using L929 cells, purified using CsCl-gradient centrifugation, and stored as diluted aliquots at -80°C (49).

Plasmids. The luciferase reporter plasmid pNF-κB-luc and internal control reporter plasmid pRenilla-luc were previously described (20). The plasmid pISRE-luc (Stratagene) encodes five tandem copies of the ISG54 interferon-stimulated response element (ISRE) 5' to a gene encoding firefly luciferase. The plasmid pIFN-β-luc was provided by John Hiscott (McGill University, Montreal, Canada). A construct expressing T3D μ2 in a pCAGGs backbone was generated previously (55). To generate pcDNA3-FLAG-μ2, the T3D M1 gene was subcloned into the *Eco*RI and *Not*I restrictions sites of pcDNA3 (Invitrogen), and a C-terminal FLAG epitope tag was inserted using the *Not*I and *Xba*I restriction sites. To generate pcDNA3-FLAG-μ2-YYFF, both tyrosine residues in the ITAM were substituted with phenylalanine using the QuikChange Site-Directed Mutagenesis Kit. To maximize μ2 and

μ2-YYFF expression (Figs. 2.2, 2.4 and 2.5), the upstream Kozak sequence was optimized by changing ACCATGG to GCCACCATGG. A plasmid expressing human Syk in a pcDNA3 backbone was a generous gift from Sheng Wei (H. Lee Moffitt Cancer Center and Research Institute, Tampa, Florida). A plasmid expressing T1L μNS in a pcDNA backbone was kindly provided by Takeshi Kobayashi while in the Dermody laboratory (Vanderbilt University School of Medicine, Nashville, Tennessee). A plasmid expressing FLAG-NS3/4A from Hepatitis C virus (HCV) in a pcDNA backbone was provided by Dr. Zhijian Chen (University of Texas Southwestern Medical Center, Dallas, Texas).

Transfections. For Fig. 2.2, each well of a 6-well cluster of AD-293 cells was transfected with all 100 μl of a reaction containing 3 μl FuGENE 6 and 1 μg of effector plasmid. For Fig. 2.3, each well of a 96-well (A) or 6-well cluster (B) of HEK-293 cells was transfected with 5 μl (A) or 100 μl (B) of a 100 μl reaction containing 6 μl FuGENE 6, 0.1 μg pRenilla-luc, 1 μg of reporter plasmid, and 1, 0.1, or 0.05 μg of effector plasmid. For Fig. 2.4, Syk was inhibited by incubating AD-293 cells in 96-well (A) or 6-well (B) clusters with 25 mM piceatannol (EMD Calbiochem) dissolved in DMSO (Sigma-Aldrich), or DMSO alone as a control (final 1% DMSO). After 1 h, AD-293 cells were transfected using 10 μl (96-well) or 100 μl (6-well) of a 200 μl reaction. For 96-well clusters, each 200 μl reaction contained 3 μl Lipofectamine 2000 (Life Technologies), 0.1 μg pRenilla-luc, 1 μg reporter plasmid, and 0.1 ug of effector plasmid. For 6-well clusters, each 200 μl reaction contained 3 μl Lipofectamine 2000, 1 μg pRenilla-luc, and 1 ug of effector plasmid. For Fig. 2.5, each chamber of 8-chamber slides of Vero cells was transfected with 60 μl of a 100 μl reaction containing 3 μl FuGENE 6, 0.025 μg Syk, 1 μg pcDNA3-μNS, and 1 μg of effector plasmid.

For Fig. 2.6A, each well of a 96-well cluster of AD-293 cells was transfected with 5 μl of a 100 μl reaction contained 3 μl FuGENE 6, 0.1 μg pRenilla-luc, and 1 μg pNF-κB-luc. At 24 h post-transfection, AD-293 cells were washed twice with media, infected, incubated for 1 h at 37°C, supplemented with media, and incubated as indicated.

Luciferase assay. Transfected cells in 96-well clusters were lysed, and luciferase activity was determined using a dual luciferase reporter assay system (Promega) according to the manufacturer's instructions. Luciferase activity for each sample was normalized to the internal *Renilla* luciferase control, and replicate wells were averaged and standard errors of the mean were determined.

Antibodies for Western blot analysis. Antibodies were used at the indicated final dilutions and purchased from the following suppliers: mouse monoclonal anti-FLAG M2 (1:1,000; Agilent Technologies, no. 200472-21) (Fig. 2.2), mouse monoclonal anti-FLAG M2 (1:2,500; Sigma-Aldrich, no. F3165) (Fig. 2.3), rabbit polyclonal anti-μ2 (1:500; generated against two μ2 peptides by Open Biosystems), mouse monoclonal anti-phosphotyrosine 4G10 (1:1000; Millipore, no. 05-321), goat polyclonal HRP-conjugated anti-GAPDH (1:160; Santa Cruz Biotechnology, no. sc-20357-HRP), goat polyclonal HRP-conjugated anti-Actin (1:500, Santa Cruz Biotechnology, no. sc-1615), polyclonal HRP-conjugated goat anti-mouse (1:2,000; Millipore, no. 12-349), and polyclonal HRP-conjugated goat anti-rabbit (1:2,000; Millipore, no. AP132P).

SDS-PAGE and immunoblotting. Transfected cells in 6-well clusters were lysed to generate total cellular protein extracts using RIPA lysis buffer (50 mM Tris HCl [pH 7.4], 1% NP-40, 0.25% sodium deoxycholate, 150 mM NaCl, 1 mM EDTA) supplemented to

contain 1% sodium dodecylsulfate (SDS) and a cocktail of protease and phosphatase inhibitors (Sigma-Aldrich). Cells were rocked on ice for 15 min and centrifuged at 10,000 x *g* for 10 min at 4°C to remove cellular debris. Protein concentrations were determined using a bicinchoninic acid protein assay (Thermo Fisher Scientific), and 10-30 μg of protein from each lysate was boiled for 5 min in 1x Laemmli sample buffer and resolved using 10% SDS-polyacrylamide gel electrophoresis (SDS-PAGE). The resolved proteins were transferred to nitrocellulose (Whatman, Protran 0.45μm pore size) in transfer buffer (48mM Tris, 39mM glycine, 0.04% SDS, and 20% methanol) for 45 minutes at 15 volts in a semi-dry transfer apparatus (Bio-Rad; Trans-Blot SD). Following protein transfer, membranes were blocked for 1 h with 3-5% milk or 5% BSA (Sigma-Aldrich) in Tris-buffered saline (20 mM Tris HCL [pH7.6], 137 mM NaCl) containing 0.05-0.1% Tween 20 (TBS-T), and probed with the indicated primary antibodies overnight at 4°C. Membranes were washed three times with TBS-T buffer, followed by 90 min incubation with the appropriate HRP-conjugated, species-specific secondary antibodies at room temperature. Membranes were washed and proteins were visualized using Amersham enhanced chemiluminescence (ECL) or ECL Plus kits (GE Healthcare) according to the manufacturer's instructions. Membranes were exposed to film and converted to digital format using an HP Scanjet G4050; quantification of the digitized bands was determined using UN-SCAN-IT software (Silk Scientific).

Immunoprecipitation. Transfected cells in 6-well clusters were lysed using Cell Lysis Buffer (Cell Signaling Technology) containing a cocktail of protease and phosphatase inhibitors (Sigma-Aldrich). Cells were rocked on ice for 10 min, sonicated, and centrifuged at 14,000 x *g* for 10 min at 4°C to remove cellular debris. Protein concentrations were

determined using a bicinchoninic acid protein assay (Thermo Fisher Scientific). 600 µg of cell lysate was added to EZview Red anti-FLAG M2 Affinity Gel (Sigma-Aldrich) according to the manufacturer's instructions and incubated overnight at 4° while rotating. After centrifugation at 8,200 x *g* for 1 min, the supernatant was removed and beads were washed three times with ice-cold TBSX (20 mM Tris HCL [pH7.6], 137 mM NaCl, 2mM ETDA, 1% Triton-X 100). Following the final wash, beads were resuspended in 50 µl of 2X laemmli sample buffer, boiled for 5 minutes, and centrifuged at 8,200 x *g* for 1 min. The supernatant was removed and subjected to 7.5% SDS-PAGE.

Quantification of viral replication. . L929 cells, primary cardiac myocyte cultures, or AD-293 cells were plated in 96-well clusters and infected at the indicated multiplicity of infection (MOI). After 1 h incubation at 37°C, additional medium with or without anti-IFN-β antibody (640 neutralizing units/ml; PBL, no. 32400-1) was added to each well, and cells were incubated for various intervals with or without additional anti-IFN-β antibody (640 neutralizing units/ml at 2 days post-infection) before freezing at -80°C. Cells were subjected to two additional freeze-thaw cycles and subsequently lysed in 0.5% NP-40. Viral titers were determined by plaque assay using L929 cells (45).

Assessment of cytopathic effect. L929 cells or primary cardiac myocyte cultures were plated in 96-well clusters and infected at the indicated MOI. After 1 h incubation at 37°C, additional medium was added to each well. At 24 h, 5 days, or 7 days post-infection, cell viability was quantified using an MTT assay (48). Absorbance was determined by subtracting OD at 650 nm from OD at 570 nm using an automated microplate reader (TECAN Sunrise Microplate Reader).

Quantitative (real-time) reverse transcription-PCR (qRT-PCR). Cells in 24-well (L929 cells) or 48-well (primary cardiac myocyte cultures) clusters were infected, incubated for 1 h, supplemented with media, and then incubated as indicated. Total RNA was harvested using an RNeasy kit (Qiagen) and treated with RNase-free DNase I (Qiagen). One-third of the RNA from each well was used to generate cDNA by reverse transcription in 100 μl containing 5 μM oligo(dT) (Invitrogen), 1X Taq buffer (Promega), 7.5 mM MgCl2 (Promega), 1 mM dithiothreitol (Promega), 1 mM each deoxynucleoside triphosphate (Roche), 0.67 U/μl RNasin (Promega), and 0.20 U/μl AMV reverse transcriptase (Promega). Five percent of the resultant cDNA was amplified using an iCycler iQ Real-Time PCR Detection System (Bio-Rad Laboratories) in 96-well plates. Each duplicate 25 μl reaction contained 1X Quantitech SYBR Green master mix (Qiagen), 10 mM fluorescein, and 0.3 μM of each forward and reverse primer. Primer sequences were as previously published (50). Relative abundance of IFN-β and GAPDH mRNA was determined by comparison to a standard curve generated from serial dilutions of a DNA standard, and IFN-β expression was normalized to GAPDH expression.

Indirect immunofluorescence and confocal microscopy. Transfected Vero cells in 8-well collagen-coated chamber slides were fixed in 2% paraformaldehyde (Electron Microscopy Sciences) and permeabilized with 0.01% Triton X-100 in phosphate-buffered saline (PBS) for 5 min at room temperature. Slides were then rinsed in PBS and blocked with 5% normal goat serum (Sigma-Aldrich) diluted in PBS for 30 min at room temperature. Cells were probed sequentially using a rabbit polyclonal anti-μ2 antibody (1:600) and a mouse monoclonal anti-Syk (1:500, Millipore, no. 05-434) diluted in 0.01% IgG- and protease-free

bovine serum albumin (BSA) (Jackson ImmunoResearch Laboratories, Inc.) for 30 min each. Samples were washed three times in PBS and sequentially incubated with Alexa 488-conjugated goat anti-rabbit IgG (1:1,000; Invitrogen) and Alexa 594-conjugated goat anti-mouse IgG (1:1,000; Invitrogen) secondary antibodies for 30 min each to detect μ2 and Syk, respectively. Samples were washed three times in PBS, and coverslips were mounted on slides using ProLong Gold reagent (Invitrogen). Images were obtained using a Zeiss Laser Scanning Confocal Microscope 710 equipped with a 40X C-apochromat / 1.1 NA water immersion objective. The pinhole was maintained at 1 AU (40 μm), and images were taken using sequential scanning. Alexa Fluor 488 was excited at 488 nm using a multiline argon laser and emission was detected in the 492 and 560 nm range. Alexa Fluor 594 was excited at 561 nm with a 561 diode pumped solid state laser and emission was detected in the 593 and 696 nm range. Images were processed and prepared for presentation using Adobe Photoshop CS4.

Statistical analysis. A Student's two-sample *t* test (pooled variance) was applied using Systat 9.0 software. Results were considered significant if the *P* value was < 0.05.

RESULTS

ITAM sequences are identified in three reovirus proteins. The protein sequences encoded by each of the 10 reovirus gene segments were screened for potential ITAM sequences using the consensus motif YxxI/L$x_{(6-12)}$YxxI/L (51). Remarkably, ITAM

sequences were identified in three reovirus proteins: σ2 (amino acids [aa] 130-147), μ2 (aa 118-134), and λ2 (aa 671-684) encoded by the S2, M1, and L2 gene segments, respectively (Fig. 2.1A). ITAM sequences were not identified in a search of the related *Reoviridae* virus, rotavirus. ITAM sequences in the reovirus σ2, μ2, and λ2 proteins were identical among prototype strains type 1 Lang (T1L), type 2 Jones (T2J), and type 3 Dearing (T3D). However, variability was evident in the T2J sequences immediately adjacent to the ITAM sequences. A clustal alignment of the μ2 ITAM sequence with corresponding motifs from DAP12, FcRγ, and CD3ζ family members demonstrated conservation of the ITAM as well as acidic residues in μ2 that are common to many cellular ITAMs (Fig. 2.1B). Conservation of critical residues in the motif across reovirus serotypes suggests a role for ITAMs in viral replication and pathogenesis. Given the previously established role of μ2 in modulating the IFN response and myocarditis in a mouse model, we focused on the ITAM sequence in μ2 first (22, 55).

μ2 is phosphorylated on multiple tyrosine residues. Phosphorylation of critical tyrosine residues is a fundamental step in ITAM-mediated signaling (51). To determine whether the μ2 ITAM is equipped for similar signal transduction, we examined the phosphorylation status of μ2 tyrosine residues in FLAG-tagged μ2 and a derivative in which the two canonical ITAM tyrosine residues in μ2 were exchanged with phenylalanine residues (YYFF). Tyrosine-to-phenylalanine substitutions were chosen to prevent the phosphorylation required for ITAM function and to minimally alter protein structure given the similarity of the tyrosine and phenylalanine side chains. These substitutions did not compromise overall μ2 structure and function as evidenced by the replication-competence of similarly substituted

whole viruses (see below). AD-293 cells were transfected with plasmids expressing FLAG-tagged μ2, FLAG-tagged μ2-YYFF, or FLAG-tagged NS3/4A, a negative control for tyrosine phosphorylation. Whole cell lysates were immunoprecipitated, and fractions resolved by SDS-PAGE were immunoblotted using anti-FLAG or anti-phosphotyrosine antibodies (Fig. 2.2). No antiphosphotyrosine-reactive bands were seen for FLAG-NS3/4A, though it was well expressed and immunoprecipitated. Notably, both FLAG-μ2 and FLAG-μ2-YYFF were found to be phosphorylated on tyrosine residues, providing the first evidence that μ2 is a phosphorylated protein. However, μ2 contains 30 tyrosines, and the significant phosphorylation of FLAG-μ2-YYFF suggests that multiple residues outside of the ITAM sequence are phosphorylated. This abundant μ2 phosphorylation precluded detection of possible decreased phosphorylation in FLAG-μ2-YYFF relative to FLAG-μ2, leaving the status of tyrosine phosphorylation in the μ2 ITAM sequence unclear.

NF-κB is activated by μ2 and maximal activation requires the μ2 ITAM. NF-κB is a well-documented downstream target of ITAM-mediated signaling (18, 23). To determine the capacity of μ2 to activate NF-κB, HEK-293 cells were transfected with FLAG-μ2 or FLAG-μ2-YYFF, and after 24 h, NF-κB-stimulated luciferase reporter gene expression was quantified (Fig. 2.3A). Over-expressed FLAG-μ2 activated NF-κB, providing the first evidence that reovirus protein μ2 can activate NF-κB. In sharp contrast, FLAG-μ2-YYFF activation of NF-κB was minimal or undetectable, demonstrating a biochemical link between the μ2 ITAM and NF-κB activation. As a control, μ2 expression levels in cell lysates generated from replicate cultures were quantified (Fig. 2.3B). Even when levels of FLAG-μ2-YYFF protein were greater than five-fold higher than those of FLAG-μ2 protein, FLAG-

μ2-YYFF activation of NF-κB was undetectable or significantly less than that by FLAG-μ2 (compare 1 μg μ2-YYFF to 0.1 μg μ2). Finally, neither FLAG-μ2 nor FLAG-μ2-YYFF induced IFN-β or the IFN-stimulated pathway as monitored by an ISRE reporter (Fig. 2.3A). These results are consistent with a requirement for viral activation of IRF3 for induction of IFN-β and highlight the specific effect of the μ2 ITAM on activation of NF-κB.

μ2 requires Syk for maximal activation of NF-κB. Activation of NF-κB through ITAM-mediated signaling requires Syk (or in T-cells, Zap-70) (3, 40). To determine whether μ2 signal transduction is mediated through classical ITAM signaling intermediates, we examined the requirement for Syk in μ2 activation of NF-κB (Fig. 2.4A). AD-293 cells were pretreated with DMSO alone or with the Syk-specific inhibitor piceatannol before transfection with plasmids encoding either FLAG-tagged or untagged μ2. After 24 h, NF-κB-stimulated luciferase reporter gene expression was quantified. A 2.5-2.9-fold decrease in μ2 activation of NF-κB was observed in the presence of piceatannol, demonstrating a requirement for Syk in μ2-mediated signal transduction. μ2 was expressed at equivalent levels in DMSO and piceatannol-treated lysates (Fig. 2.4B), demonstrating that reduced μ2 activation of NF-κB was due to depletion of Syk rather than decreased μ2 expression. Thus, μ2 contains a functional ITAM that signals through an established ITAM-associated signaling intermediate to activate NF-κB.

μ2 recruits Syk to viral factories and recruitment requires the μ2 ITAM. Reovirus protein μ2 does not span membranes, suggesting it functions in a manner that differs from other viral and cellular ITAM-containing proteins (32, 51). While μ2 is found in low copy number within the viral core, μ2 is abundant and highly concentrated in reovirus

infected cells within cytoplasmic viral replication-associated structures known as viral factories (VFs, also known as viral inclusion bodies or VIBs) (10, 42). Though VFs are thought to lack a delimiting membrane, we hypothesized they may serve as intracellular sites for μ2 ITAM interaction with Syk. To determine the effect of the μ2 ITAM on Syk cellular localization, we employed confocal microscopy to visualize Vero cells cotransfected with plasmids expressing Syk, reovirus protein μNS to induce VF formation (4, 38), and either FLAG-pcDNA3, FLAG-μ2, or FLAG-μ2-YYFF (Fig. 2.5). We used Vero cells rather than AD-293 cells due to their larger cytoplasm and capacity to form more defined viral factories. In cells expressing FLAG-pcDNA3 or FLAG-μ2-YYFF, Syk remained diffuse throughout the cell, despite adequate formation of VFs in the latter. Conversely, in cells expressing FLAG-μ2, Syk was localized to VFs. Thus, μ2 recruits Syk to VFs and recruitment requires the μ2 ITAM, representing a novel mechanism for viral ITAM-mediated signaling.

The μ2 ITAM regulates activation of NF-κB during viral infection. Reovirus activates NF-κB during infection, mediating apoptosis in the brain and an antiviral IFN response in the heart (41). To investigate the role of ITAMs in reovirus infection, plasmid-based reverse genetics was employed to engineer wild-type (WT) reovirus strain T3D and mutant viruses. Mutant viruses with altered ITAMs in the λ2 protein could not be recovered despite three independent rescue attempts. However, viruses with altered σ2 (σ2-YYFF) or μ2 (μ2-YYFF) ITAMs were readily isolated and formed plaques similar in size to WT virus (data not shown). To determine whether the μ2 ITAM regulates activation of NF-κB in the context of reovirus infection, AD-293 cells were cotransfected with the NF-κB-luciferase reporter plasmid and Renilla-luciferase plasmid as before, and then infected with WT T3D,

σ2-YYFF, or μ2-YYFF viruses. At 12 h post-infection, WT T3D and σ2-YYFF viruses activated NF- κB, but μ2-YYFF did not (Fig. 2.6A). While μ2-YYFF achieved titers intermediate to those of WT T3D and σ2-YYFF viruses at 12 h post-infection (Fig. 2.6B), it remained possible that differences in NF-κB activation might reflect differences in replication. However, even at 24 h post-infection when μ2-YYFF achieved titers similar or equal to those of WT T3D and σ2-YYFF (Fig. 2.6B), μ2-YYFF failed to activate NF-κB as efficiently as either virus (Fig. 2.6A). Therefore, decreased activation of NF-κB by reovirus mutant μ2-YYFF does not reflect diminished viral replication, but instead reflects the requirement for the μ2 ITAM for maximal activation of NF-κB during reovirus infection.

The μ2 ITAM regulates induction of IFN-β. Viral activation of NF-κB is required for maximal induction of IFN-β, and the IFN-β response is a critical determinant of protection against reovirus-induced myocarditis in a mouse model (13, 22, 48). To determine whether the μ2 ITAM modulates reovirus induction of IFN-β, non-specialized L929 cells or primary cardiac myocyte cultures were infected with WT T3D and mutant reoviruses, and induction of IFN-β mRNA was examined. In both L929 cells and primary cardiac myocyte cultures, μ2-YYFF induced significantly less IFN-β than did either WT T3D or σ2-YYFF viruses (Fig. 2.7A), despite replicating to similar titers (Fig. 2.7B). Thus, the μ2 ITAM regulates the induction of IFN-β.

The μ2 ITAM effect on viral spread is cell type-specific. Viral spread is determined by an overlapping network of virus and host cell interactions involving viral replication, virus-induced cytopathicity, and virus-induced anti-viral cytokines. To determine the effect of the μ2 ITAM on viral spread, L929 cells and primary cardiac myocyte cultures

were infected at a low MOI with WT T3D, σ2-YYFF, or μ2-YYFF viruses and incubated for 5 to 7 days to allow multiple cycles of viral replication. In L929 cells, all three viruses achieved equivalent viral titers (Fig. 2.8A), however, μ2-YYFF was significantly less cytopathic than either WT T3D or σ2-YYFF viruses at both 5 and 7 days post-infection (Fig. 2.9). These data suggest that in L929 cells, where NF-κB is required for reovirus-mediated apoptosis (41), the μ2 ITAM is advantageous for viral spread. In contrast to L929 cells, μ2-YYFF achieved a significantly higher titer than either WT T3D or σ2-YYFF viruses in primary cardiac myocyte cultures (Fig 2.8A). Inclusion of anti-IFN-β antibody during infection increased replication of both WT T3D and σ2-YYFF viruses to levels similar to μ2-YYFF in cardiac myocyte cultures, but had no impact on viral titer in L929 cells (Fig 2.8B). Thus the effect of the μ2 ITAM on viral spread was mediated by the IFN-β response and was cell type-specific. Finally, again in contrast to L929 cells, μ2-YYFF was significantly more cytopathic than either WT T3D or σ2-YYFF in primary cardiac myocyte cultures (Fig. 2.9). Therefore, in cardiac myocytes, where the IFN response is critical to limit viral damage and NF-κB is not required for apoptosis (19, 41, 48), the μ2 ITAM stimulates cellular defense mechanisms, subsequently diminishing viral replication and spread. Thus the overall effect of the μ2 ITAM on reovirus replication and cytopathology is cell type-specific.

DISCUSSION

In this study, we identify ITAM sequences in reovirus proteins μ2, σ2, and λ2 (Fig. 2.1). We demonstrate that the ITAM in the M1 gene-encoded μ2 protein requires Syk for μ2-mediated signal transduction, and regulates activation of NF-κB and induction of IFN-β in a cell type-specific manner. Furthermore, we provide evidence of a novel mechanism for viral ITAM-mediated signaling by a nonenveloped virus.

The two critical tyrosine residues within the canonical ITAM motif $YxxI/Lx_{6-12}YxxI/L$ must be phosphorylated for efficient recruitment of Syk tyrosine kinases and activation of ITAM-mediated signaling cascades (51). Here we demonstrate that μ2 undergoes extensive tyrosine phosphorylation, providing the first evidence that μ2 is a phosphorylated protein (Fig. 2.2). However, phosphorylation of μ2-YYFF in the context of thirty tyrosine residues prevented concluding whether ITAM tyrosines are phosphorylated.

ITAM tyrosine phosphorylation is dependent on Src family kinase members including Src, Lck, Lyn, Fgr, Hck, Fyn, and Yes, some of which are expressed in only certain cell types. Furthermore, viral ITAMs have been shown to display cell type-specific kinase associations. The Epstein-Barr virus (EBV) LMP2A ITAM is phosphorylated by Csk in epithelial cells but preferentially associates with Lyn and Fyn in BJAB cells, a B cell line (5, 44). Reovirus infects a wide variety of tissues *in vivo*, including the brain, heart, liver, intestine, and spleen (10). Future investigations will determine whether associations of Src family kinases with the μ2 ITAM varies between cell types and influences the capacity of the μ2 ITAM to modulate cell signaling.

Here we demonstrate that NF- κB, a well-documented downstream target of ITAM-mediated signaling (18, 51), is activated by μ2 and that maximal activation requires the μ2 ITAM (Fig. 2.3). Additionally, ectopically expressed μ2 does not activate IFN-β or ISRE luciferase reporters (Fig. 2.3), consistent with the expected requirement for MAVS-dependent transcription factors such as IRF3 and confirming the specificity of the μ2 effect on NF- κB. While previous investigations have implicated reovirus protein μ1 in NF-κB activation, results presented here for μ2 suggest reovirus regulates NF-κB activation through multiple viral effectors (6). Reovirus NF-κB activation requires components of both the classical and alternative NF-κB signaling pathways in an integrated mechanism involving IKKα and the IKKβ regulatory protein NEMO/IKKγ, but not IKKβ or the IKKα activator NIK (20). It has been hypothesized that reovirus μ1 φ domain may contribute to NF-κB activation through direct or indirect stimulation of IKKs in a fashion similar to that seen during human T-lymphotropic virus (HTLV) infection, where the HTLV Tax protein stimulates IKK activity though direct interaction with NEMO/IKKγ (8). In the case of μ2, activation of NF-κB requires ITAM-mediated signaling intermediates.

We demonstrate that μ2 requires Syk for maximal activation of NF-κB (Fig. 2.4), providing evidence that μ2 contains a functional ITAM capable of signaling through an established ITAM-associated signaling intermediate. Syk tyrosine kinases have been found to mediate signal transduction for several viral ITAMs including EBV LMP2A (36), KSHV K1 (30, 33), mouse mammary tumor virus (MMTV) envelope protein (Env) (43), Hantavirus G1 (16, 17), and SIV Nef (9, 37). However, as a nonenveloped viral protein, reovirus protein μ2 does not associate with cellular membranes, suggesting it stimulates Syk activation and

downstream signaling cascades in a manner that differs from other cellular and viral ITAM-containing protein. LMP2A is a highly hydrophobic protein containing twelve transmembrane domains and is localized within aggregates to the plasma membrane of latently infected B cells. The recruitment of kinases to LMP2A ITAM residues for tyrosine phosphorylation is stimulated through cellular adhesion rather than ligand binding as classically demonstrated by ITAM-associated proteins (44). The KSHV K1 ITAM is located within the cytoplasmic tail of the transmembrane protein and is able to constitutively induce signal transduction through ligand-independent activation attributed to the K1 cysteine-rich extracellular domain (31, 34). In this study we provide evidence that μ2 ITAM signaling is stimulated through a novel mechanism involving recruitment of Syk to cytoplasmic viral replication-associated structures. The structure of μ2 has not been solved, but the ITAM identified here is located directly adjacent to a μ2 sequence predicted to have the greatest likelihood of localization to the protein surface, consistent with a model of direct interaction between the μ2 ITAM and the Syk SH2 domain (53).

During reovirus infection, replication and assembly of reovirus progeny occurs within cytoplasmic viral factories (VFs), also known as viral inclusion bodies. Reovirus protein μNS initiates VF formation by establishing a structural matrix and acting as a scaffolding protein for recruitment of μ2, S3-encoded nonstructural protein σNS, and core structural proteins (4, 38, 39). VFs become tethered to the cellular cytoskeleton via μNS associations with the microtubule-associated μ2. This association allows VFs to travel toward the nucleus and merge with other VFs, ultimately forming the large perinuclear inclusions characteristic of reovirus infected cells (38, 42). Here we demonstrate that μ2, a major component of VFs,

recruits Syk to viral factories and that the μ2 ITAM is required for this translocation (Fig. 2.5). While VFs are thought to lack a delimiting membrane, further investigation on the structural composition of VFs may identify properties of VFs that support μ2 ITAM-Syk interaction. Furthermore, Syk has been shown to phosphorylate microtubules (12). Given that reovirus protein μ2 binds microtubules (4), future investigations will address whether microtubules play a role in μ2 ITAM-Syk interactions.

During reovirus infection, NF-κB mediates reovirus-induced apoptosis and subsequent pathogenesis in a cell type-specific manner. NF-κB plays a proapoptotic role in the brain, stimulating neuronal apoptosis following reovirus infection, while in the heart NF-κB is not required for apoptosis and activation leads to induction of innate immune mediators including IFN-β (41). Here, we found that the μ2 ITAM was required for maximal activation of NF-κB and induction of IFN-β in both L929 cells and primary cardiac myocyte cultures (Fig. 2.7), but that the consequences to viral cytopathic effect and spread are cell type-specific (Figs. 2.8, 2.9). Together, these data suggest that in L929 cells where NF-κB is required for reovirus-induced apoptosis, the μ2 ITAM is advantageous for viral spread and enhances viral fitness. In cardiac myocytes where IFN-β is critical for protection against reovirus replication and cytopathic effects and NF-κB is not required for apoptosis, the μ2 ITAM stimulates cellular defense mechanisms and thereby diminishes viral fitness (19, 41, 48).

Several enveloped viruses encode ITAM-bearing proteins that participate in viral pathogenesis and oncogenesis through mediation of traditional cellular ITAM signaling intermediates (32). During Epstein-Barr virus (EBV) infection, Syk regulates EBV LMP2A

ITAM-induced epithelial cell migration through activation of MAPK extracellular signal-regulated kinase (ERK) (36). Recent studies also identified the ITAM-bearing protein as essential for ERK-mediated reduction of anoikis, a type of apoptosis associated with cell detachment (24). Finally, LMP2A ITAM-mediated Syk autophosphorylation initiates Akt activation, a serine/threonine protein kinase involved in cellular survival and proliferation signaling cascades that contributes to B cell survival and is required for LMP2A-induced transformation of epithelial cells (14). In the Kaposi's sarcoma-associated herpesvirus (KSHV) K1 ITAM, each tyrosine residue targets distinct SH2-containing proteins including PI3K, PLCγ2, and Vav. This leads to regulated augmentation of signal transduction activities involved in KS hyperplasia such as intracellular calcium mobilization, activation of transcription factors NFAT and AP-1, and production of inflammatory cytokines and angiogenic growth factors (33). Additionally, the simian immunodeficiency virus (SIV) Nef ITAM was found to be necessary and sufficient for Lck activation of NFAT, a key downstream intermediate of T cell activation (9, 37). While presented results here demonstrated that the μ2 ITAM stimulates Syk activation of NF-κB, it remains entirely possible that μ2 stimulation of Syk activates other transcription factors as well.

Viral ITAMs are most often associated with oncogenesis. In EBV, the ITAM-bearing viral protein LMP2A has been implicated in maintenance of viral latency through interference of B cell receptor signaling, which in turn blocks viral reactivation. LMP2A also contributes to the malignant phenotypes seen in both B cells and epithelial cells through manipulation of cellular networks involved in transformation, migration, and differentiation (14). Unlike most cancers which are caused by clonal expansion of transformed cells,

KSHV-induced Kaposi's Sarcoma (KS) is a result of hyperplastic growth associated with local production of inflammatory cytokines. The KSHV K1 ITAM targets distinct SH2-containing proteins leading to augmentation of specific signal transduction activities involved in KS hyperplasia such as intracellular calcium mobilization, activation of NFAT and AP-1 transcription factors, and production of inflammatory cytokines and angiogenic growth factors (33). Activation of NFAT by another herpesvirus, rhesus monkey rhadinovirus (RRV), is also mediated by an ITAM, in this case, RRV R1 (7). The MMTV Env ITAM is a mediator of epithelial cell transformation, and mutation of critical tyrosine residues abrogates Env signaling, resulting in altered mammary epithelial cell transformation and attenuated tumorigenesis (27, 43). Finally, bovine leukemia virus (BLV) contains two ITAMs that are critical for BLV infection, propagation, and signal transduction (2, 52).

Reovirus is not oncogenic. Currently, there are two non-oncogenic viruses reported to encode ITAM containing proteins: hantavirus and SIV. The hantavirus G1 ITAM is highly conserved in hantavirus strains causing hantavirus pulmonary syndrome but absent in those causing hemorrhagic fever with renal syndrome or nonpathogenic strains, suggesting that this viral ITAM is a determinant of pathogenesis. In SIV, the primary pathogenic-determinant of a highly virulent isolate was identified to be an arginine to tyrosine mutation within the viral protein Nef that caused Nef to express a functional ITAM (9, 37). The cell type-specific effects of the reovirus μ2 ITAM identified here suggest that it is likely to be a determinant of pathogenesis *in vivo*, and the capacity of reovirus to target a variety of organs in the mouse offers a tremendous opportunity for discovery.

As a final note, an ITAM-like sequence has been identified in only one non-enveloped virus to date: coxsackievirus. However, substitution of critical tyrosine residues within the ITAM-like region of capsid protein VP2 attenuated the virus used in these studies, leaving interpretation of the results presented on ITAM function unclear (26).

Results presented here define a new role for reovirus protein μ2 and enhance our understanding of reovirus-mediated activation of NF- κB and induction of IFN-β. Furthermore, we provide evidence for the first functional ITAM in a nonenveloped virus, and present a novel mechanism for viral ITAM-mediated signaling.

ACKNOWLEDGMENTS

We thank Ralph Baric, Lianna Li, Ray Pickles, Frank Scholle, Jennifer Zurney and, Kim Parks for helpful discussions and Lance Johnson for excellent technical assistance. This research was supported by Public Health Service awards T32 CA09385 (K.W.B.), F32 AI075776 (K.W.B.), R37 AI38296 (T.S.D.), R01 AI50080 (T.S.D.), and R01 A1083333 (B.S.) and the Elizabeth B. Lamb Center for Pediatric Research. Additional support was provided by Public Health Service awards CA68485 for the Vanderbilt-Ingram Cancer Center and DK20593 for the Vanderbilt Diabetes Research and Training Center.

REFERENCES

1. **Baty, C. J., and B. Sherry.** 1993. Cytopathogenic effect in cardiac myocytes but not in cardiac fibroblasts is correlated with reovirus-induced acute myocarditis. Journal of virology **67:**6295-6298.

2. **Beaufils, P., D. Choquet, R. Z. Mamoun, and B. Malissen.** 1993. The (YXXL/I)2 signalling motif found in the cytoplasmic segments of the bovine leukaemia virus envelope protein and Epstein-Barr virus latent membrane protein 2A can elicit early and late lymphocyte activation events. The EMBO journal **12:**5105-5112.

3. **Bradshaw, J. M.** 2010. The Src, Syk, and Tec family kinases: distinct types of molecular switches. Cellular signalling **22:**1175-1184.

4. **Broering, T. J., J. S. Parker, P. L. Joyce, J. Kim, and M. L. Nibert.** 2002. Mammalian reovirus nonstructural protein microNS forms large inclusions and colocalizes with reovirus microtubule-associated protein micro2 in transfected cells. Journal of virology **76:**8285-8297.

5. **Burkhardt, A. L., J. B. Bolen, E. Kieff, and R. Longnecker.** 1992. An Epstein-Barr virus transformation-associated membrane protein interacts with src family tyrosine kinases. Journal of virology **66:**5161-5167.

6. **Coffey, C. M., A. Sheh, I. S. Kim, K. Chandran, M. L. Nibert, and J. S. Parker.** 2006. Reovirus outer capsid protein micro1 induces apoptosis and associates with lipid droplets, endoplasmic reticulum, and mitochondria. Journal of virology **80:**8422-8438.

7. **Damania, B., M. DeMaria, J. U. Jung, and R. C. Desrosiers.** 2000. Activation of lymphocyte signaling by the R1 protein of rhesus monkey rhadinovirus. Journal of virology **74:**2721-2730.

8. **Danthi, P., C. M. Coffey, J. S. Parker, T. W. Abel, and T. S. Dermody.** 2008. Independent regulation of reovirus membrane penetration and apoptosis by the mu1 phi domain. PLoS pathogens **4:**e1000248.

9. **Dehghani, H., C. R. Brown, R. Plishka, A. Buckler-White, and V. M. Hirsch.** 2002. The ITAM in Nef influences acute pathogenesis of AIDS-inducing simian immunodeficiency viruses SIVsm and SIVagm without altering kinetics or extent of viremia. Journal of virology **76:**4379-4389.

10. **Dermody, T. S., J. Parker, B. Sherry.** 2013. Orthoreoviruses, p. 1304-1346. *In* D. M. K. a. P. M. Howley (ed.), Fields Virology, 6th ed, vol. 2. Wolters Kluwer Health/Lippincott Williams & Wilkins, Philadelphia.

11. **Dermody, T. S., L. A. Schiff, M. L. Nibert, K. M. Coombs, and B. N. Fields.** 1991. The S2 gene nucleotide sequences of prototype strains of the three reovirus serotypes: characterization of reovirus core protein sigma 2. Journal of virology **65:**5721-5731.

12. **Faruki, S., R. L. Geahlen, and D. J. Asai.** 2000. Syk-dependent phosphorylation of microtubules in activated B-lymphocytes. Journal of cell science **113 (Pt 14):**2557-2565.

13. **Fensterl, V., and G. C. Sen.** 2009. Interferons and viral infections. Biofactors **35:**14-20.

14. **Fotheringham, J. A., N. E. Coalson, and N. Raab-Traub.** 2012. Epstein-Barr virus latent membrane protein-2A induces ITAM/Syk- and Akt-dependent epithelial migration through alphav-integrin membrane translocation. Journal of virology **86:**10308-10320.

15. **Fredericksen, B. L., B. C. Keller, J. Fornek, M. G. Katze, and M. Gale, Jr.** 2008. Establishment and maintenance of the innate antiviral response to West Nile Virus involves both RIG-I and MDA5 signaling through IPS-1. Journal of virology **82:**609-616.

16. **Geimonen, E., I. Fernandez, I. N. Gavrilovskaya, and E. R. Mackow.** 2003. Tyrosine residues direct the ubiquitination and degradation of the NY-1 hantavirus G1 cytoplasmic tail. Journal of virology **77:**10760-10868.

17. **Geimonen, E., R. LaMonica, K. Springer, Y. Farooqui, I. N. Gavrilovskaya, and E. R. Mackow.** 2003. Hantavirus pulmonary syndrome-associated hantaviruses contain conserved and functional ITAM signaling elements. Journal of virology **77:**1638-1643.

18. **Hara, H., C. Ishihara, A. Takeuchi, L. Xue, S. W. Morris, J. M. Penninger, H. Yoshida, and T. Saito.** 2008. Cell type-specific regulation of ITAM-mediated NF-kappaB activation by the adaptors, CARMA1 and CARD9. J Immunol **181:**918-930.

19. **Holm, G. H., A. J. Pruijssers, L. Li, P. Danthi, B. Sherry, and T. S. Dermody.** 2010. Interferon regulatory factor 3 attenuates reovirus myocarditis and contributes to viral clearance. Journal of virology **84:**6900-6908.

20. **Holm, G. H., J. Zurney, V. Tumilasci, S. Leveille, P. Danthi, J. Hiscott, B. Sherry, and T. S. Dermody.** 2007. Retinoic acid-inducible gene-I and interferon-

beta promoter stimulator-1 augment proapoptotic responses following mammalian reovirus infection via interferon regulatory factor-3. The Journal of biological chemistry **282:**21953-21961.

21. **Humphrey, M. B., L. L. Lanier, and M. C. Nakamura.** 2005. Role of ITAM-containing adapter proteins and their receptors in the immune system and bone. Immunological reviews **208:**50-65.

22. **Irvin, S. C., J. Zurney, L. S. Ooms, J. D. Chappell, T. S. Dermody, and B. Sherry.** 2012. A single-amino-acid polymorphism in reovirus protein mu2 determines repression of interferon signaling and modulates myocarditis. Journal of virology **86:**2302-2311.

23. **Ivashkiv, L. B.** 2009. Cross-regulation of signaling by ITAM-associated receptors. Nature immunology **10:**340-347.

24. **Iwakiri, D., T. Minamitani, and M. Samanta.** 2013. Epstein-Barr Virus Latent Membrane Protein 2A Contributes to Anoikis Resistance through ERK Activation. Journal of virology **87:**8227-8234.

25. **Kato, H., O. Takeuchi, E. Mikamo-Satoh, R. Hirai, T. Kawai, K. Matsushita, A. Hiiragi, T. S. Dermody, T. Fujita, and S. Akira.** 2008. Length-dependent recognition of double-stranded ribonucleic acids by retinoic acid-inducible gene-I and melanoma differentiation-associated gene 5. The Journal of experimental medicine **205:**1601-1610.

26. **Kim, D. S., J. H. Park, J. Y. Kim, D. Kim, and J. H. Nam.** 2012. A mechanism of immunoreceptor tyrosine-based activation motif (ITAM)-like sequences in the capsid protein VP2 in viral growth and pathogenesis of Coxsackievirus B3. Virus genes **44:**176-182.

27. **Kim, H. H., S. M. Grande, J. G. Monroe, and S. R. Ross.** 2012. Mouse mammary tumor virus suppresses apoptosis of mammary epithelial cells through ITAM-mediated signaling. Journal of virology **86:**13232-13240.

28. **Kobayashi, T., A. A. Antar, K. W. Boehme, P. Danthi, E. A. Eby, K. M. Guglielmi, G. H. Holm, E. M. Johnson, M. S. Maginnis, S. Naik, W. B. Skelton, J. D. Wetzel, G. J. Wilson, J. D. Chappell, and T. S. Dermody.** 2007. A plasmid-based reverse genetics system for animal double-stranded RNA viruses. Cell host & microbe **1:**147-157.

29. **Kobayashi, T., L. S. Ooms, M. Ikizler, J. D. Chappell, and T. S. Dermody.** 2010. An improved reverse genetics system for mammalian orthoreoviruses. Virology **398:**194-200.

30. **Lagunoff, M., D. M. Lukac, and D. Ganem.** 2001. Immunoreceptor tyrosine-based activation motif-dependent signaling by Kaposi's sarcoma-associated herpesvirus K1 protein: effects on lytic viral replication. Journal of virology **75:**5891-5898.

31. **Lagunoff, M., R. Majeti, A. Weiss, and D. Ganem.** 1999. Deregulated signal transduction by the K1 gene product of Kaposi's sarcoma-associated herpesvirus. Proceedings of the National Academy of Sciences of the United States of America **96:**5704-5709.

32. **Lanier, L. L.** 2006. Viral immunoreceptor tyrosine-based activation motif (ITAM)-mediated signaling in cell transformation and cancer. Trends in cell biology **16:**388-390.

33. **Lee, B. S., S. H. Lee, P. Feng, H. Chang, N. H. Cho, and J. U. Jung.** 2005. Characterization of the Kaposi's sarcoma-associated herpesvirus K1 signalosome. Journal of virology **79:**12173-12184.

34. **Lee, H., J. Guo, M. Li, J. K. Choi, M. DeMaria, M. Rosenzweig, and J. U. Jung.** 1998. Identification of an immunoreceptor tyrosine-based activation motif of K1 transforming protein of Kaposi's sarcoma-associated herpesvirus. Molecular and cellular biology **18:**5219-5228.

35. **Loo, Y. M., J. Fornek, N. Crochet, G. Bajwa, O. Perwitasari, L. Martinez-Sobrido, S. Akira, M. A. Gill, A. Garcia-Sastre, M. G. Katze, and M. Gale, Jr.** 2008. Distinct RIG-I and MDA5 signaling by RNA viruses in innate immunity. Journal of virology **82:**335-345.

36. **Lu, J., W. H. Lin, S. Y. Chen, R. Longnecker, S. C. Tsai, C. L. Chen, and C. H. Tsai.** 2006. Syk tyrosine kinase mediates Epstein-Barr virus latent membrane protein 2A-induced cell migration in epithelial cells. The Journal of biological chemistry **281:**8806-8814.

37. **Luo, W., and B. M. Peterlin.** 1997. Activation of the T-cell receptor signaling pathway by Nef from an aggressive strain of simian immunodeficiency virus. Journal of virology **71:**9531-9537.

38. **Miller, C. L., M. M. Arnold, T. J. Broering, C. E. Hastings, and M. L. Nibert.** 2010. Localization of mammalian orthoreovirus proteins to cytoplasmic factory-like structures via nonoverlapping regions of microNS. Journal of virology **84:**867-882.

39. **Miller, C. L., T. J. Broering, J. S. Parker, M. M. Arnold, and M. L. Nibert.** 2003. Reovirus sigma NS protein localizes to inclusions through an association requiring the mu NS amino terminus. Journal of virology **77:**4566-4576.

40. **Mocsai, A., J. Ruland, and V. L. Tybulewicz.** 2010. The SYK tyrosine kinase: a crucial player in diverse biological functions. Nature reviews. Immunology **10:**387-402.

41. **O'Donnell, S. M., M. W. Hansberger, J. L. Connolly, J. D. Chappell, M. J. Watson, J. M. Pierce, J. D. Wetzel, W. Han, E. S. Barton, J. C. Forrest, T. Valyi-Nagy, F. E. Yull, T. S. Blackwell, J. N. Rottman, B. Sherry, and T. S. Dermody.** 2005. Organ-specific roles for transcription factor NF-kappaB in reovirus-induced apoptosis and disease. The Journal of clinical investigation **115:**2341-2350.

42. **Parker, J. S., T. J. Broering, J. Kim, D. E. Higgins, and M. L. Nibert.** 2002. Reovirus core protein mu2 determines the filamentous morphology of viral inclusion bodies by interacting with and stabilizing microtubules. Journal of virology **76:**4483-4496.

43. **Ross, S. R., J. W. Schmidt, E. Katz, L. Cappelli, S. Hultine, P. Gimotty, and J. G. Monroe.** 2006. An immunoreceptor tyrosine activation motif in the mouse mammary tumor virus envelope protein plays a role in virus-induced mammary tumors. Journal of virology **80:**9000-9008.

44. **Scholle, F., R. Longnecker, and N. Raab-Traub.** 1999. Epithelial cell adhesion to extracellular matrix proteins induces tyrosine phosphorylation of the Epstein-Barr virus latent membrane protein 2: a role for C-terminal Src kinase. Journal of virology **73:**4767-4775.

45. **Sherry, B., C. J. Baty, and M. A. Blum.** 1996. Reovirus-induced acute myocarditis in mice correlates with viral RNA synthesis rather than generation of infectious virus in cardiac myocytes. Journal of virology **70:**6709-6715.

46. **Sherry, B., and M. A. Blum.** 1994. Multiple viral core proteins are determinants of reovirus-induced acute myocarditis. Journal of virology **68:**8461-8465.

47. **Sherry, B., and B. N. Fields.** 1989. The reovirus M1 gene, encoding a viral core protein, is associated with the myocarditic phenotype of a reovirus variant. Journal of virology **63:**4850-4856.

48. **Sherry, B., J. Torres, and M. A. Blum.** 1998. Reovirus induction of and sensitivity to beta interferon in cardiac myocyte cultures correlate with induction of myocarditis and are determined by viral core proteins. Journal of virology **72:**1314-1323.

49. **Smith, R. E., H. J. Zweerink, and W. K. Joklik.** 1969. Polypeptide components of virions, top component and cores of reovirus type 3. Virology **39:**791-810.

50. **Stewart, M. J., K. Smoak, M. A. Blum, and B. Sherry.** 2005. Basal and reovirus-induced beta interferon (IFN-beta) and IFN-beta-stimulated gene expression are cell type specific in the cardiac protective response. Journal of virology **79:**2979-2987.

51. **Underhill, D. M., and H. S. Goodridge.** 2007. The many faces of ITAMs. Trends in immunology **28:**66-73.

52. **Willems, F., F. Andris, D. Xu, D. Abramowicz, M. Wissing, M. Goldman, and O. Leo.** 1995. The induction of human T cell unresponsiveness by soluble anti-CD3 mAb requires T cell activation. International immunology **7:**1593-1598.

53. **Yin, P., N. D. Keirstead, T. J. Broering, M. M. Arnold, J. S. Parker, M. L. Nibert, and K. M. Coombs.** 2004. Comparisons of the M1 genome segments and encoded mu2 proteins of different reovirus isolates. Virology journal **1:**6.

54. **Zurney, J., K. E. Howard, and B. Sherry.** 2007. Basal expression levels of IFNAR and Jak-STAT components are determinants of cell-type-specific differences in cardiac antiviral responses. Journal of virology **81:**13668-13680.

55. **Zurney, J., T. Kobayashi, G. H. Holm, T. S. Dermody, and B. Sherry.** 2009. Reovirus mu2 protein inhibits interferon signaling through a novel mechanism involving nuclear accumulation of interferon regulatory factor 9. Journal of virology **83:**2178-2187.

A

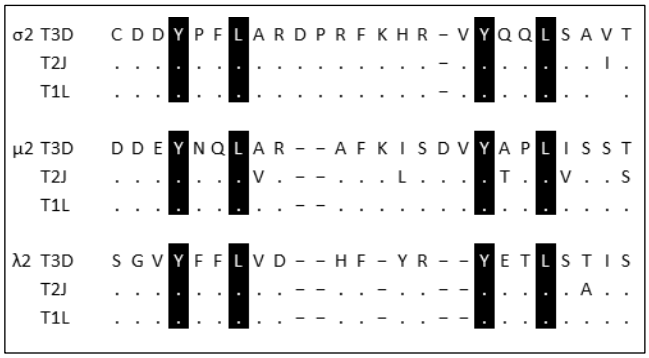

B

Species	Protein	Sequence
T3D	μ2	D D E Y N Q L A R A F K I S D V Y A P L I S S T
T2J	μ2	D D E Y N Q L V R A F K L S D V Y T P L V S S S
T1L	μ2	D D E Y N Q L A R A F K I S D V Y A P L I S S T
Hs	DAP12	E S P Y Q E L Q - G - Q R S D V Y S D L N T Q R
Mm	Dap12	E S P Y Q E L Q - G - Q R P E V Y S D L N T Q R
Dr	Dap12	E S P Y Q E L Y - G - V Q S D I Y S D L Q Q Y R
Dr	CD3ζL2	E T H Y Q E L R - A - H A S D E Y Q Q I G T K G
Hs	FcRγ	D G V Y T G L S - T - R N Q E T Y E T L K H E K
Mm	FcRγ	D A V Y T G L N - T - R S Q E T Y E T L K H E K
Xl	FcRγ	E G E Y T G L E - S - V D K G T Y E T I K G E S
Dr	FcRγ	E G V Y E G L K - P - H E T D T Y E T I K M K S
Hs	CD3ζ3	D G L Y Q G L S - T - A T K D T Y D A L H M Q A
Mm	CD3ζ3	D G L Y Q G L S - T - A T K D T Y D A L H M Q T
Dr	CD3ζ3	D Q L Y Q G L S - S - V T K D T Y D S L Q M Q Q
Xl	CD3ζ3	D P V Y Q G L H - S - G S R D T Y D A L H M Q P
Gg	CD3ζ3	D A V Y Q G L S - A - A T R D T Y D A L H M Q P
Dr	FcRγL	G D L Y Q D L G - R - R D A D T Y D T L H G M K
Dr	CD3ζ2	D E T Y T P L T - R - K G D D T Y R E L E T K G
Hs	CD3ζ1	N Q L Y N E L N - L - G R R E E Y D V L D K R R
Mm	CD3ζ1	N Q L Y N E L N - L - G R R E E Y D V L E K K R
Gg	CD3ζ1	D D V Y N K L S - R - G H R D E Y D V L G T R R
Xl	CD3ζ1	D N N Y D E L N - P - S G Q S K Y D A L N V R R
Hs	CD3ζ2	E G L Y N E L Q - K D K M A E A Y S E I G M K G
Mm	CD3ζ2	E G V Y N A L Q - K D K M A E A Y S E I G T K G
Gg	CD3ζ2	D T V Y S S L Q - K D K M G E A Y S E I G K K G
Xl	CD3ζ2	D S T Y T G L Q - R D K M S D P Y S D I R P K Q
Dr	CD3ζ1	E S H Y Q A I D - K - L G K S E Y A T A N R T Q
Dr	CD3ζL1	E P V Y T D L D - L P Q V G S D Y Q Q L D R P I

Figure 2.1. ITAM sequences identified in three reovirus proteins. (A) ITAMs in the reovirus σ2, μ2, and λ2 proteins. ITAMs of prototype reovirus strains T3D, T2J, and T1L are shown. Sequences are from (11,15, 53). (B) Reovirus μ2 ITAMs aligned with cellular ITAMs. Black indicates conserved ITAM residues. Grey indicates additional residues common to many ITAMs. Hs = *Homo sapiens* (human); Mm = *Mus musculus* (mouse); Dr = *Danio rerio* (zebrafish); Xl = *Xenopus laevis*; Gg = *Gallus gallus* (chicken). The extensions 1, 2, and 3 following protein names distinguish between the three ITAMs in each of the indicated proteins.

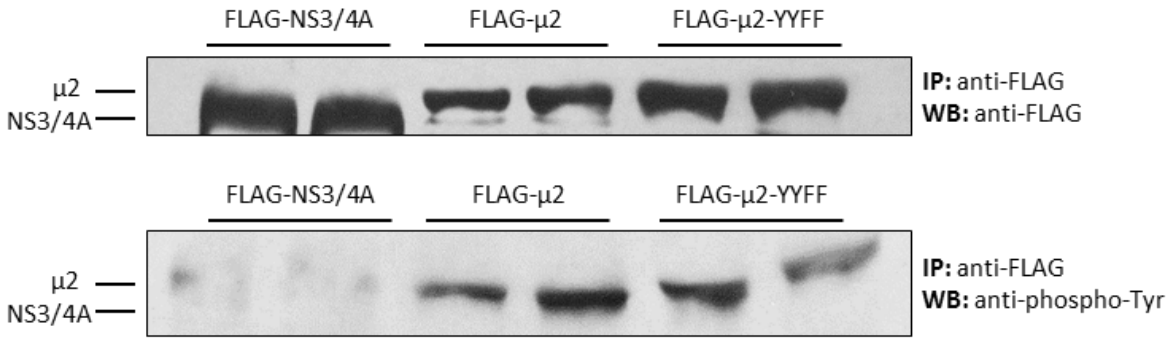

Figure 2.2. μ2 is phosphorylated on multiple tyrosine residues. AD-293 cells were transfected with the indicated FLAG-tagged plasmid. At 40 h post-transfection, whole-cell lysates were immunoprecipitated using anti-FLAG beads and fractions from duplicate IPs were resolved by SDS-PAGE and immunoblotted using anti-FLAG (Agilent) or anti-phosphotyrosine antibodies. Results are representative of at least two independent experiments.

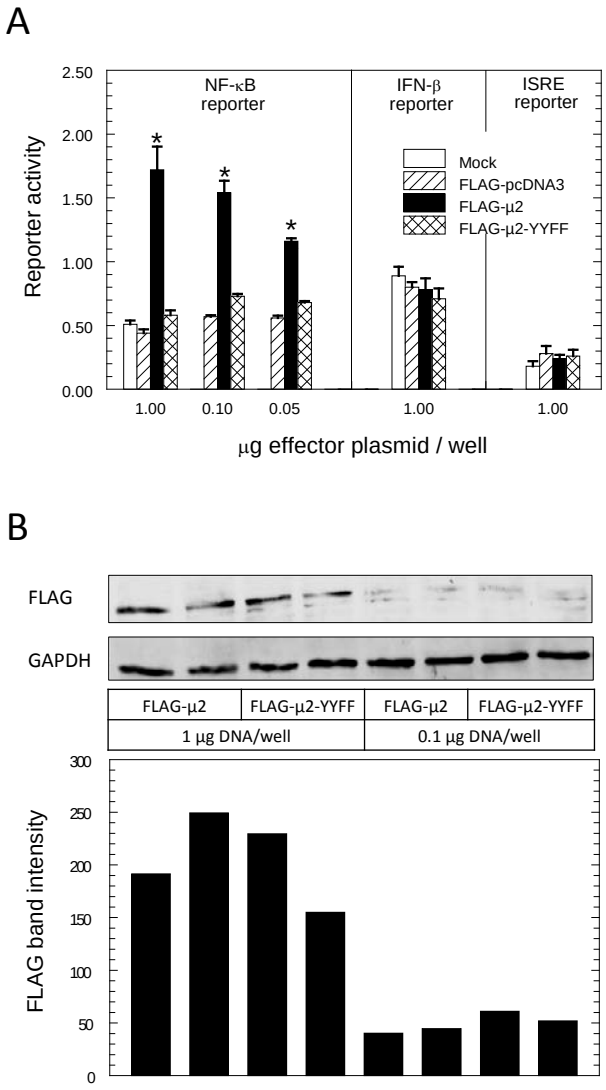

Figure 2.3. NF-κB is activated by μ2 and maximal activation requires the μ2 ITAM. (A) HEK-293 cells were cotransfected with the indicated FLAG-tagged plasmid, a constitutively-expressing Renilla-luciferase plasmid for normalizations, and a lucife rase reporter plasmid regulated by NF-κB, IFN-β, or ISRE promoters. At 24 h post-transfection, luciferase activity was quantified. Results are expressed as the mean ± standard error of the mean of 5 replicate samples and are representative of two independent experiments. (B) Whole-cell lysates corresponding to (A) were resolved by SDS-PAGE, transferred to a nitrocellulose membrane, and immunoblotted using anti-FLAG or anti-GAPDH antibodies. Gels were scanned, and band intensity was quantified. Results are representative of at least two independent experiments. *, significantly different from FLAG-pcDNA3 and FLAG-μ2-YYFF ($P < 0.05$).

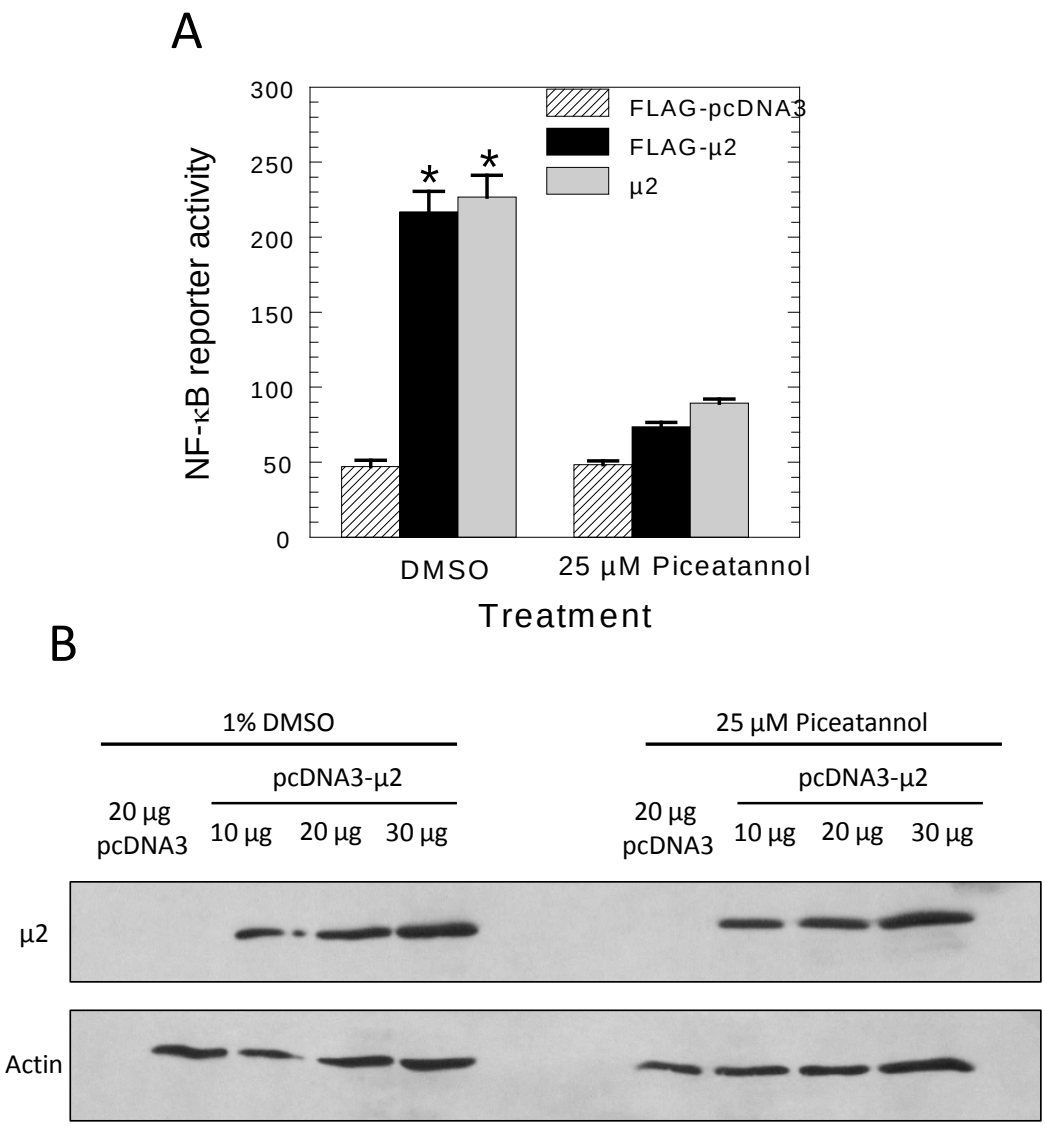

Figure 2.4. μ2 requires Syk for maximal activation of NF-κB. (A) AD-293 cells were treated for 1 h with DMSO alone or 25 μM of the Syk-specific inhibitor piceatannol and then cotransfected with the indicated effector plasmid, a constitutively-expressing Renilla-luciferase plasmid for normalizations, and an NF-κB-luciferase reporter plasmid. At 24 h post-transfection, luciferase activity was quantified. Results are expressed as the mean ± standard error of the mean of six replicate samples and are representative of at least two independent experiments. (B) Whole-cell lysates corresponding to (A) were resolved by SDS-PAGE, transferred to a nitrocellulose membrane, and immunoblotted using anti-μ2 or anti-actin-HRP antibodies. Results are representative of at least two independent experiments. *, significantly different from μ2 and μ2-YYFF in piceatannol and FLAG-pcDNA3 in either treatment ($P < 0.05$).

Figure 2.5. μ2 recruits Syk to viral factories and recruitment requires the μ2 ITAM. Vero cells were co-transfected with the indicated FLAG-tagged plasmid, μNS, and Syk. At 24 h post transfection, cells were fixed and immunolabeled with an antibody against Syk (green) and an antibody against reovirus protein μ2 (red). Results are representative of three independent experiments. Scale bar, 20 μm; Inset scale bar, 10 μm.

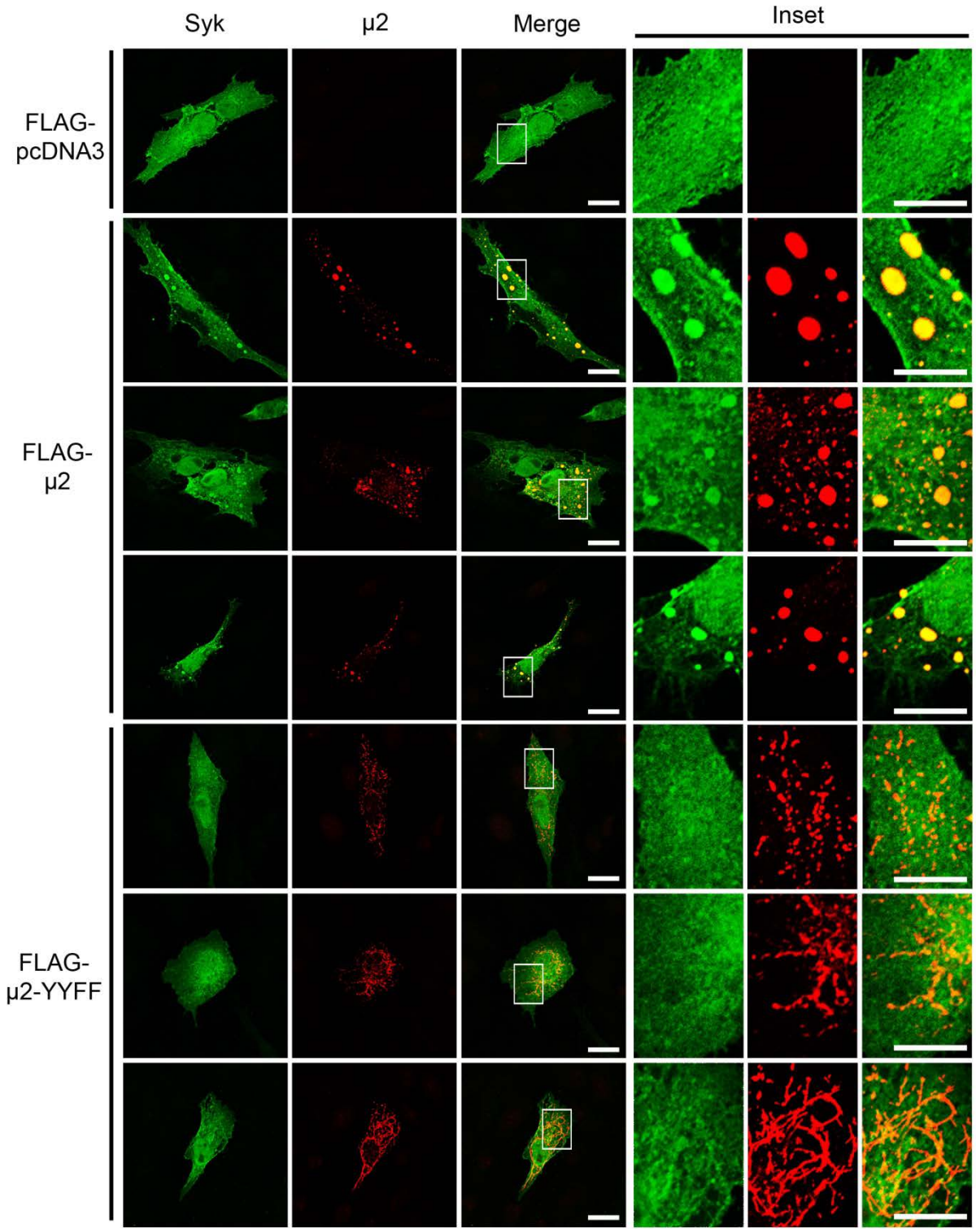
Syk
μ2
Merge
Inset
FLAG-
pcDNA3
FLAG-
μ2
FLAG-
μ2-YYFF

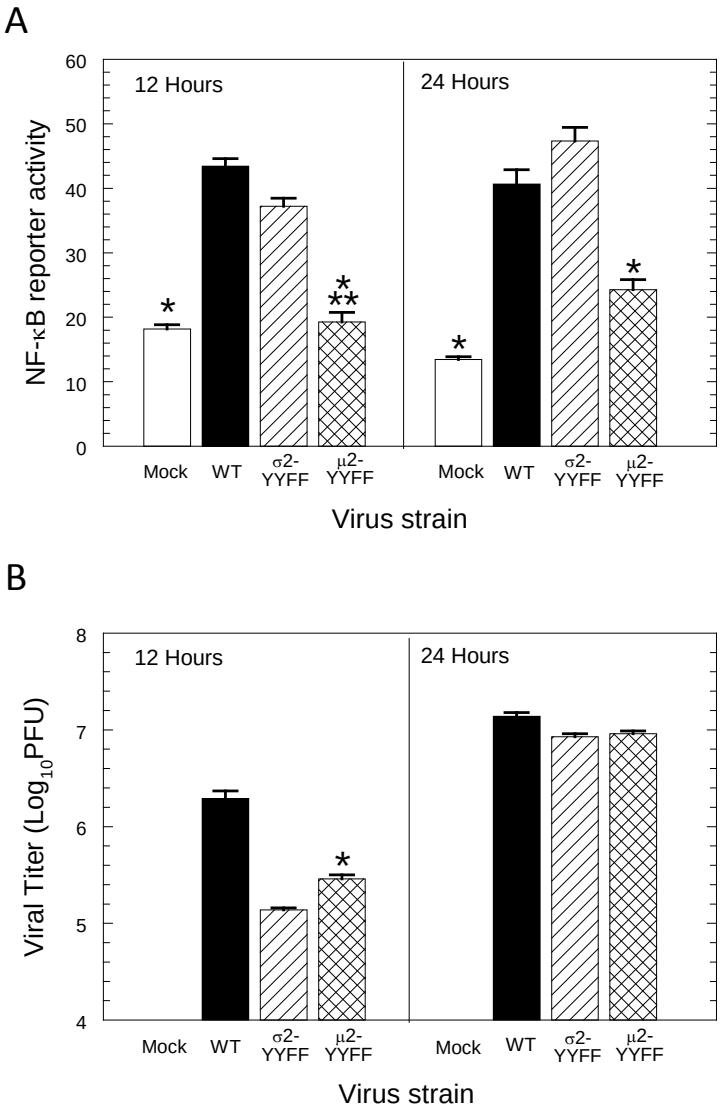

Figure 2.6. The μ2 ITAM regulates activation of NF-κB during viral infection. (A) AD-293 cells were transfected with an NF-κB-luciferase reporter plasmid and a constitutively-expressing Renilla-luciferase plasmid for normalizations. At 24 h post-transfection, cells were infected with the indicated virus at an MOI of 10 PFU per cell. At 12 and 24 h post-infection, luciferase activity was quantified. Results are expressed as the mean ± standard deviation of 4 or 5 replicate wells and are representative of at least 3 independent experiments. (B) AD-293 cells were infected with the indicated virus at an MOI of 3 PFU per cell. At 12 and 24 h post-infection, viral titers were determined by plaque assay. Results are expressed as the mean of quadruplicate samples ± standard deviation for a representative of at least two independent experiments. *, significantly different from WT T3D and σ2-YFF ($P < 0.05$); **, not significantly different from mock ($P < 0.05$).

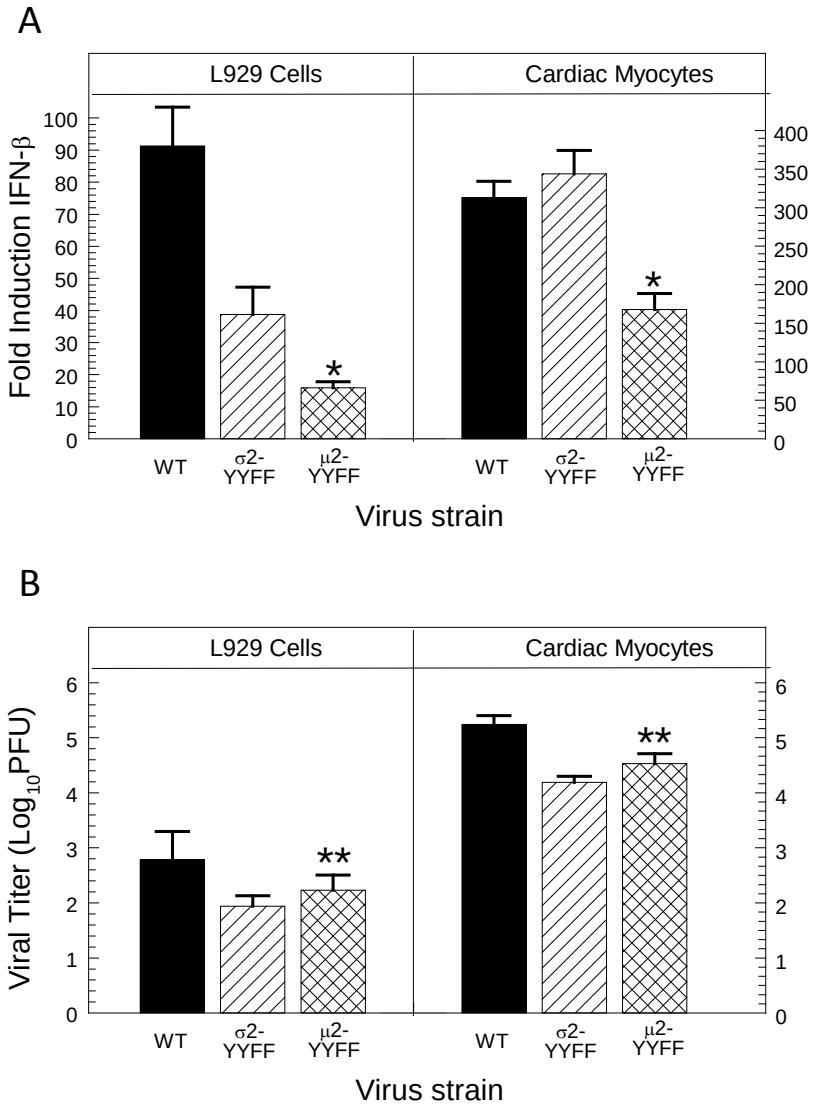

Figure 2.7. The μ2 ITAM regulates induction of IFN-β. (A) L929 cells or primary cardiac myocyte cultures were infected at an MOI of 25 or 10 PFU per cell, respectively. At 8 or 12 hr post-infection, RNA was quantified by reverse transcription and quantitative RealTime PCR, and copy number was normalized to GAPDH. Fold induction of IFN-β is expressed relative to mock-infected cultures. Results are expressed as the mean ± standard error of the mean of triplicate wells for a representative of three independent experiments. (B) L929 cells or primary cardiac myocytes cultures were infected with the indicated virus at an MOI of 3 PFU per cell. At 8 h post infection, viral titers were determined by plaque assay. Results are expressed as the mean ± standard deviation for for two or three independent experiments each with triplicate wells. *, significantly different from WT T3D and σ2-YFF ($P < 0.05$). **, significantly different from σ2-YFF ($P < 0.05$).

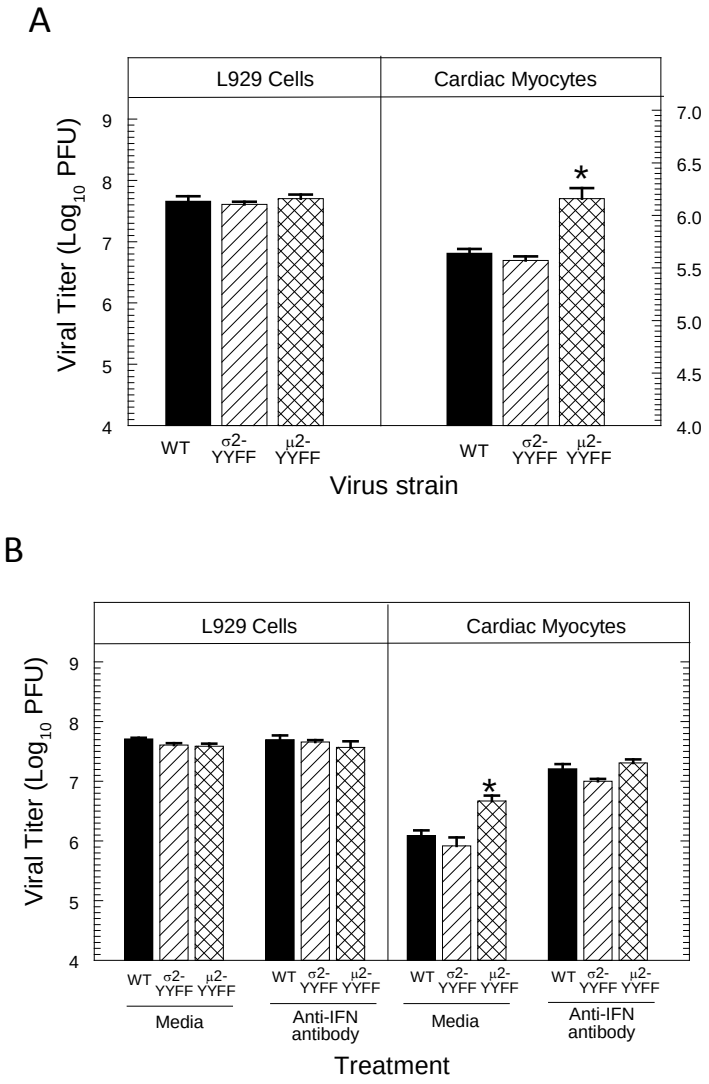

Figure 2.8. The impact of the μ2 ITAM on viral titer after multiple cycles of replication is cell type-specific and is determined by the IFN-β response. (A) L929 cells and primary cardiac myocyte cultures were infected with the indicated virus at an MOI of 0.1 PFU per cell. At 5 days post-infection, viral titers were determined by plaque assay. Results are expressed as the mean ± standard deviation of triplicate wells for a representative of at least two independent experiments. (B) L929 cells and primary cardiac myocyte cultures were infected at an MOI of 0.1 or 0.3 PFU per cell, respectively. At 1 h post-infection, inocula were removed and replaced with either media alone or media containing anti-IFN-beta antibody. At 2 days post-infection, additional anti-IFN-beta antibody was added to appropriate wells. Results are expressed as the mean of quadruplicate samples ± standard deviation for a representative of at least two independent experiments. *, significantly different from WT T3D and σ2-YFF ($P < 0.05$).

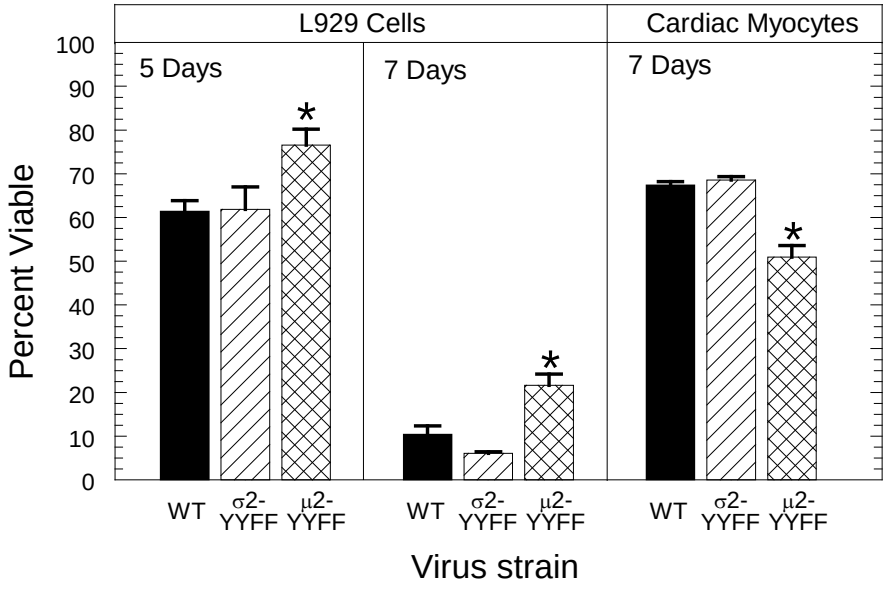

Figure 2.9. The impact of the μ2 ITAM on cytopathic effect after multiple cycles of replication is cell type-specific. L929 cells or primary cardiac myocyte cultures were infected with the indicated virus at an MOI of 0.1 or 1 PFU per cell, respectively (cytopathic effect was undetectable in cardiac myocytes infected at 0.1 PFU per cell; data not shown). At 5 and 7 days post-infection, cell viability was quantified by MTT assay. Results from a minimum of four replicate wells per infection are expressed as the mean ± standard error of the mean relative to mock-infected cultures for a representative of at least two independent experiments. *, significantly different from WT T3D and σ2-YYFF ($P < 0.05$).